

## SURVEY OF SECULAR RESONANCES IN THE ASTEROID BELT

Z. Knežević

*Serbian Academy of Sciences and Arts,  
Kneza Mihaila 35, 11000 Belgrade, Serbia*

E-mail: [zoran.knezevic@sanu.ac.rs](mailto:zoran.knezevic@sanu.ac.rs)

(Received: September 3, 2021; Accepted: September 3, 2021)

**SUMMARY:** Using a recently introduced synthetic method to compute the asteroid secular frequencies (Knežević and Milani 2019), in this paper we survey the locations of secular resonances in the 9 dynamically distinct zones of the asteroid belt. Positions of all resonances up to order four, of a significant fraction of the order six resonances, and of a several order eight ones were determined, plotted in the space of proper elements, and discussed in relation to the local dynamics and to the structure and shape of the nearby asteroid collisional families. Only the resonant combinations with fundamental frequencies of Jupiter and Saturn were considered, with a few special cases involving other planets and largest asteroids. Accuracy of the polynomial fit to determine the frequencies was found to be satisfactory for the purpose of determination of secular resonance positions. This enabled a precise identification of dynamical mechanisms affecting the computation of frequencies (close vicinity of the mean motion resonances and libration in secular resonances), and of the “cycle slips” as a primary technical drawback causing deterioration of the results. For each zone we also presented and discussed a fairly complete sample of recent works dealing with interaction of the secular resonances with asteroid families present in that zone. Finally, a few words were devoted to possibilities for future work.

**Key words.** Celestial mechanics – Minor planets, asteroids: general

### 1. INTRODUCTION

The importance of secular resonances for the dynamics of asteroids in general, and for the dynamical constraining of the Asteroid Main Belt in particular, has been recognized since the seminal paper by Williams and Faulkner (1981) in which *linear* secular resonances were introduced and their approximate locations determined. In that paper the surfaces for the three strongest secular resonances have been located as a function of proper semimajor axis, eccentricity, and inclination for semimajor axes between 1.25 and 3.5 AU, and it was found that “the  $\nu_5$  resonance only occurs at high inclinations ( $\geq 23^\circ$ )”, that

“the  $\nu_6$  resonance passes through both the main belt and Mars-crossing space”, and that “the  $\nu_{16}$  resonance starts near the inner edge of the belt and, at low inclinations at least, folds around a portion of the Mars-crossing space until it runs nearly parallel with the Earth-crossing boundary.”

The *nonlinear* secular resonances have in turn been introduced by Milani and Knežević (1990), who also revealed their interaction with asteroid families (see Fig. 8 of that paper), of which some characteristic examples (e.g. Eos, Lydia) were later presented in Milani and Knežević (1992) and Milani and Knežević (1994). Subsequently, the other authors followed, thus the literature on the subject is at present abundant indeed. The first survey of the positions of linear secular resonances in the Solar System planetary region, from 2 to 50 au, has been made by Knežević et al. (1991), followed by the survey of resonances below 2 au by Michel and Froeschlé (1997).

---

© 2022 The Author(s). Published by Astronomical Observatory of Belgrade and Faculty of Mathematics, University of Belgrade. This open access article is distributed under CC BY-NC-ND 4.0 International licence.

In the recently published paper (Knežević and Milani 2019), hereinafter referred to as Review I, a new, purely numerical (*synthetic*), method to compute asteroid secular frequencies and determine the locations of secular resonances in the phase space of proper elements has been introduced. The method is closely related to a similar procedure, proposed in Milani (1994), intended to locate the secular resonances in the Trojan region. In this context, it also makes part of a continuous effort at improvement of the accuracy and long term stability of asteroid synthetic proper elements and frequencies; for some recent advances in the field see Knežević (2017).

The method consists of a polynomial fit to the perihelion and node frequencies ( $g, s$ ) of asteroids included in the current synthetic proper elements catalog, of subsequent computation of values of frequencies on a grid in the proper elements phase space, and of plotting of the interpolated contour lines corresponding to some small values of the resonant frequency combinations to visualize the resonance locations. The least squares procedure to compute the coefficients of the polynomial expressions representing frequencies is applied to the catalog frequencies of asteroids in a given dynamical zone, with the degree of the fitting polynomial and the other relevant parameters selected to suit the local dynamics.

We defined 9 dynamical zones, each covering a range in semimajor axis delimited by the most important mean motion resonances (MMRs), and selected in such a way to ensure that the dynamics within a given zone is uniform enough to justify the use of the same procedure and fit parameters in the entire zone (see Table 1 of Review I). The number of asteroids per zone is therefore different (see Table 2 of Review I), but always large enough for the purpose of computing reliably the coefficients of the fitting polynomial. In order to achieve better accuracy of the fit, these numbers are actually somewhat reduced by removal of the chaotic asteroids (Lyapunov times shorter than 50,000 y, in Zone 1 shorter than 100,000 y) and of asteroids affected by the mean motion resonances (standard deviation of proper semimajor axis  $\sigma(a) > 0.0003$  au), for which secular frequencies are known to be poorly determined. In addition, in Zone 4, all the asteroids with  $\sigma(e) > 0.003$  or  $\sigma(\sin I) > 0.003$ , affected by the nonlinear secular resonances, are also removed, in particular those affected by a strong secular resonance  $g + g_5 - 2g_6$ . In all the zones the upper bounds in terms of  $(e, \sin I)$  were defined in such a way to exclude asteroids with extremely large values of these elements (leading, for example, to close encounters with perturbing planets), and in Zones 3 and 4 we also set lower bound ( $\sin I = 0.01$ ) to avoid a few asteroids with extremely low inclinations. When setting these boundaries we took care that all the resonances of interest are included in the zone. Eventually, we thus ended up with 6485 asteroids in the least populous Zone 1, and 91,772 asteroids in the most populous Zone 3. Note

that in both, Review I and the present review, we made use of the catalog of synthetic proper elements with 535,396 asteroids, available from the AstDyS site<sup>1</sup>.

The fitting polynomial was expressed in terms of the suitably normalized variables  $(x, y, z)$ , corresponding to proper elements  $(a, e, \sin I)$ , with values in the (0,1) range. The degree of the polynomial in terms of  $(y, z)$  was either 4 or 6, depending on the zone, with 24 and 40 terms, respectively (see Table 3 in Review I). Monomials in terms of the normalized proper semimajor axis  $x$  were mostly given up to degree 3, but up to degree 5 in Zones 4 and 9.

In order to illustrate the basic functionality and performance of the new method, in Review I we presented the results for a couple of selected zones only, namely, for dynamically distinct Zones 4 and 7. We found that “the accuracy of the fit is good enough even in the dynamically very complex zones of the asteroid main belt”, and that the method provides reliable secular resonance positions, thus being capable of fully replacing the previously available, but less accurate analytical one (Milani and Knežević 1990, 1992, 1994, Knežević et al. 1991).

In the present review, the purpose is to give a complete overview of the results for all the zones, placing emphasis on the zones with more complex dynamics and exhibiting important interactions of the secular resonances and local families. The analysis carried out here follows the main lines of Review I, in terms of the applied procedures and of the presentation of principal results, accompanied with the discussion of the characteristics and peculiarities of each zone. The families are referred to following the names and the classification by size as proposed in Milani et al. (2014). In the next Section 2 we thus survey the entire asteroid belt, passing through all the distinct dynamical zones, to summarize our main results and conclusions in a brief final Section 3.

## 2. SURVEY OF THE RESONANCES

The results obtained in Review I of the application of the new method in Zones 4 and 7 were twofold: the data pertaining to the accuracy and reliability of the least squares fit, and plots revealing either the location of poorly fitted outlier asteroids, or showing the final positions of secular resonances. The accuracy of the fit has been controlled by standard deviations of coefficients of the fitting polynomial, by the corresponding signal-to-noise ratios (absolute values of the coefficients divided by their standard deviations), and by the standard deviation of the post-fit residuals (in the sense catalog frequency derived from the synthetic theory (Knežević and Milani 2000) minus frequency obtained by the fitting procedure) of frequencies of all asteroids included in the fit (see Section 4.2 of Review I). In principle, the catalog frequencies are

<sup>1</sup><https://newton.spacedys.com/astdys2/>

considered as benchmarks in this sense, since they are computed on the individual basis, specifically for every single asteroid; the frequencies obtained by fitting procedure bear a kind of "collective" signature of all asteroids involved in the computation of the coefficients of the polynomial, hence unavoidably deviating somewhat from the specific catalog values. On the other hand, the catalog frequencies may also have large errors in some dynamical circumstances (Knežević 2020), which will be erased in the fitting process by the overwhelming majority of asteroids with accurate data. In general, thus, one can say that large post-fit residuals in any case indicate that something is wrong with a given object.

The above accuracy controls were used for the data analysis in this review too. In particular, for the post-fit residuals we tested different outlier rejection criteria, trying to identify the dynamical reasons for the failures. For the sake of simplicity and space, however, we shall not give all the details for each dynamical zone. Instead, we shall select only those specific results bringing some important dynamical insight in a given case.

### 2.1. Zone 1

Zone 1 spans the innermost range in semimajor axis:  $1.800 < a < 2.000$  au, i.e. the region below the 4:1 mean motion resonance with Jupiter. It contains essentially only the Hungaria asteroids, a large population of asteroids characterized by the low-to-moderate orbital eccentricities and high inclinations. As already mentioned above, in this zone we included 6485 asteroids in the fit. The region has been rather thoroughly studied in the recent past, see e.g. McEachern et al. (2010), Čuk et al. (2014), or Lucas et al. (2019), but we shall here single out two papers which are of interest in the context of our present analysis, that is, the papers by Warner et al. (2009), and Milani et al. (2010).

In the paper by Warner et al. (2009) a comprehensive analysis of the Hungaria group of asteroids (to be distinguished from Hungaria family, which is a subsample of the group) is presented. They looked into the rotational properties of Hungarias, their taxonomical classification, size frequency distribution, population dynamics, but what interests us most is their assessment of the interaction of Yarkovsky migration of family members with the mean motion and secular resonances, giving rise to the evolution of the group structure, in particular to the spread of the group members in terms of inclination observed in the region with  $a < 1.92$  au. To explain spreading towards the higher and lower inclinations they proposed an evolutionary scenario involving Yarkovsky migration along secular resonances and listed a number of nonlinear secular resonances as possible culprits (see Novaković et al. (2015) for an instructive example of a similar evolution in the case of Hoffmeister asteroid family). They, however, did not directly compare positions of these resonances with the loca-

tions in the orbital elements space where inclination changes, as revealed from the propagation of test orbits, were taking place. Having now at our disposal both, the accurate synthetic proper elements for all the numbered and multiopposition Hungaria, and the new method to precisely locate any secular resonance in the space of these elements, we are in position to carry out analysis which could shed some more light on the proposed scenario. More precisely, we intend to plot all the resonances mentioned by Warner et al. (2009) and check whether their conjectures are consistent with the new data.

The paper by Milani et al. (2010) in many respects precedes the present one. In particular this pertains to the fact that the Hungaria region as a whole was shown to be dynamically bounded by the strong linear secular resonances and by the close approaches to Mars. The Hungaria region, as well as the Hungaria family contained within it, were also shown to be crossed by several important mean motion resonances (especially with Mars) giving rise to large changes of proper eccentricity and inclination, and by many nonlinear secular resonances affecting their accuracy. Finally, in that paper a simple and less accurate predecessor of the new synthetic method (Knežević and Milani 2019) was used to determine positions of secular resonances. Thus, at least as regards the secular resonances, here we would like to extend this previous investigation and assess in more detail and with a more complete set of more accurately located resonances, some of the issues raised in that paper (e.g. the hint on the possible existence of a secondary family; see Section 4.4 in Milani et al. (2010)).

Following the general scheme established in Review I, let us first investigate the accuracy of the polynomial fit in Zone 1. For this purpose in Table 1 we show the values used to estimate the goodness of the fit for both frequencies, or, more precisely, the data on the post fit residuals. A degree 6 polynomial was used in this zone to fit the catalog frequencies, with a total of 40 monomials (Knežević and Milani 2019).

**Table 1:** Frequency, post fit standard deviations,  $\sigma_{all}$ , for 6485 asteroids in Zone 1 used in the fit, number of asteroids with extreme residuals  $R > 10\sigma$ ;  $N10$ , the standard deviation after removal of  $N10$  outliers;  $\sigma_{10}$ , number of asteroids with large residuals  $R > 3\sigma$ ;  $N3$ ;  $\sigma_3$ , the standard deviation after removal of  $N3$  outliers. Standard deviations are in arcsec/yr.

Freq.	$\sigma_{all}$	$N10$	$\sigma_{10}$	$N3$	$\sigma_3$
$g$	0.4159	2	0.1044	6	0.0872
$s$	0.0172	0	0.0172	95	0.0152

It can be straightforwardly concluded that the accuracy of the fit for both frequencies is very good, the

one for  $s$  being still better than the corresponding fit for  $g$ . There are just 2 “pathological” cases with extreme residuals in excess of  $10\sigma$  in  $g$ , and none in  $s$ ; on the contrary, there are 6 cases with large residuals in excess of  $3\sigma$  in  $g$ , but 95 in  $s$ . Obviously, both these features are a consequence of either comparatively large standard deviation  $\sigma_{\text{all}}$  in  $g$ , due primarily to the two pathological cases, which therefore encompasses nearly all the other asteroids, including those with comparatively large residuals, or to rather small value of the standard deviation in  $s$ , where such extreme residuals do not occur.

As shown in the left panel of Fig. 1, the two pathological cases, as well as the 6 asteroids with large residuals all have very small eccentricities and, therefore, probably suffer from the *cycle slip* problem in computation of the  $g$  frequency by means of the synthetic theory (Knežević 2020). As for the frequency  $s$ , nearly all of the 95 cases with residuals above  $3\sigma$ , shown in the right panel of Fig. 1, are clustered at proper  $a > 1.95$  au, in the region crossed by at least one s-type nonlinear resonance:  $s - g_5 + g_8 - s_6$ , which is the order 4 resonance proposed by Warner et al. (2009), and involving, curiously enough, Neptune. The position of the nonlinear resonance has been computed for the value of the third, fixed proper element  $e=0.072$ , which corresponds to the median value for the zone (see Review I). This resonance can account for a good fraction of the affected cases, but not for all. Possibly, the rest is affected by an as yet unidentified resonance of higher order.

Since the boundaries and the intricate resonant structure of Zone 1 have already been shown in great detail in Figs. 8 and 11 of Milani et al. (2010), there is no need to repeat the same information here. Instead we shall concentrate on providing an answer to the question of existence of s-type resonances serving as migratory pathways for Yarkovsky-driven asteroids towards the region of lower orbital inclinations. In Fig. 2 we thus plot all the s-related resonances listed by Warner et al. (2009), plus a 4th order s-type resonance  $2s - s_4 - s_6$  shown in Fig. 11 of Milani et al. (2010). In both panels the scale of the plot is adjusted to the one in the top panel Fig. 8 of Warner et al. (2009) to facilitate the comparison.

The positions of the considered s-related resonances seem to fully corroborate the scenario of Warner et al. (2009), with a couple of additions: (i) the migrating objects do not cross a single resonance, following it for a while and then exiting from it at some lower inclination but, instead, they cross a multiplet of resonances sometimes even partially overlapping; (ii) the resonance  $s + 2g - 2g_5 - s_7$ , mentioned as potentially important, does not matter.

Another point to explain at this point is the choice of divisor values to represent resonance surfaces in our plots (see Fig. 2). Let us emphasize that these values do not represent the separatrices of the resonances, but are chosen in such a way to correspond in a relative sense to the resonance strength: in principle,

resonances of order 4 are stronger than those of order 6, hence affecting larger area in our coordinate planes and being represented with wider boundaries. Some hints in this sense can be inferred from the analysis of Carruba (2009), who found that more than 90% of the librating asteroids have frequencies within about  $\pm 0.3$  arcsec/yr from the resonance center in the case of order 4 resonance; application of the same criterion in the case of order 6 resonance (Carruba et al. 2016a) revealed that all the librating asteroids are within the range, but a closer inspection of Fig. 8 in that paper reveals that a large majority of asteroids is actually found within  $\pm 0.1$  arcsec/yr.

The case of  $g$ -type resonance  $2g - g_5 - g_6$  is specific, in the sense that this resonance is a combination of two most powerful linear resonances  $g - g_5$  and  $g - g_6$ . Also, as illustrated in Fig. 3, in Hungaria region frequency  $g$  exhibits much larger changes as a function of (large) inclination, than the frequency  $s$  as a function of (small) eccentricity. Thus nearly resonant values of frequency  $s$  persist over a larger range of eccentricity values than this is the case for frequency  $g$  over the corresponding range in (sine of) inclination. Hence, the need to use wider boundaries to represent  $g$ -type resonances in this region.

In general, if one considers also the need, which sometimes arises, to use somewhat wider boundaries for weak high order resonances simply to make them visible in the plots, one can conclude that throughout this paper we should respect some general hierarchy of the resonance widths, but that exceptions, when justified, are also acceptable.

Let us, finally, look into the problem of the putative second family (Fig. 4), allegedly located above the main Hungaria one<sup>2</sup>, at  $0.40 < \sin I < 0.45$  (see Fig. 1). Milani et al. (2010) recognize that the apparent grouping does not represent “a strong concentration”, and that “the distribution of velocity metric and of sizes does not show a V-shape”, but that “the presence of a dip in number density for  $\sin I_p$  around 0.4 appears to contradict the interpretation of this population as background.” Not having at their disposal all the tools we have now, they did not succeed in identifying a secular resonance which stretches between the main and presumed family and may be responsible for creation of the observed “dip”. In Fig. 4 we show one such resonance:  $3g - 2g_5 - g_6$ ; it is in approximately the right place (see Knežević (2020) for a thorough study of the sensitivity of computed position of secular resonance in the high inclination region), but, being of order 6, it is not clear whether in a long run it can really affect the distribution of orbital inclinations in a visible way. If it can, the only

<sup>2</sup>A strange apparently bimodal shape of the Hungaria family at the low  $a$  side can be explained by the chaining effect, a well-known drawback of the classical HCM procedure to identify the families, due in this case probably to slightly too conservative family definition implemented by the automated procedure (Knežević et al. 2014) used to determine the family membership.

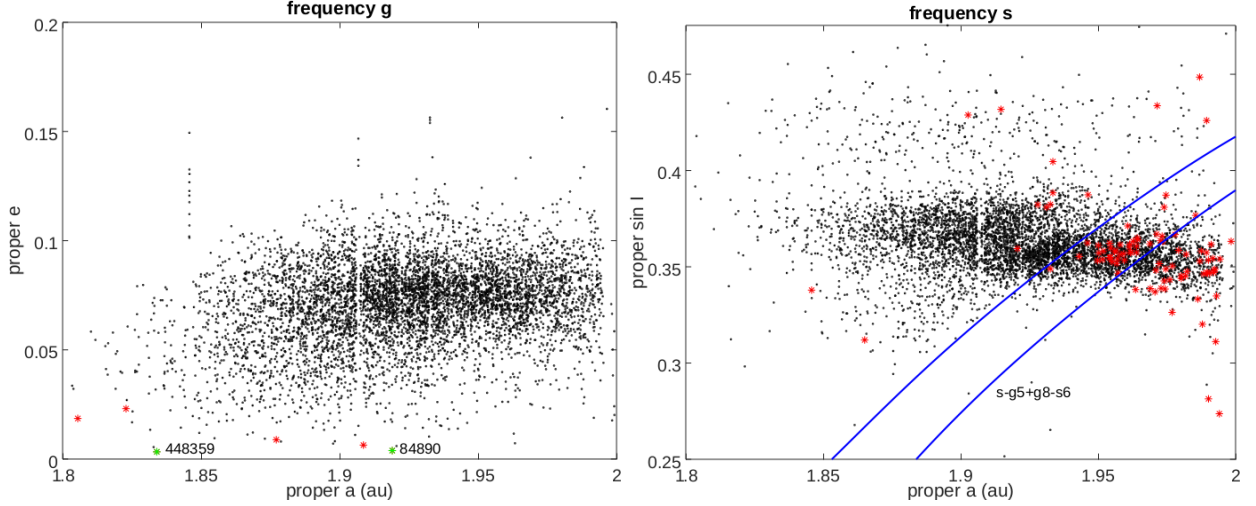


**Fig. 1:** Zone 1 in the proper  $(a, e)$ , left, and  $(a, \sin I)$  planes, right. Black dots: all the asteroids in the zone used in the fit; red asterisks: asteroids with absolute values of residuals in frequency  $g$  larger than  $3\sigma$ ; green asterisks: asteroids (84890) and (448359) with absolute values of  $g$  residuals larger than  $10\sigma$ . Vertical empty stripes are due to the pre-fit removal of chaotic asteroids and asteroids with large errors of proper semimajor axis. The nonlinear resonance  $s - g_5 + g_8 - s_6$  is represented in the right panel by the contour lines corresponding to  $(-0.3, 0.3)$  arcsec/yr values of the resonant divisor; the resonance appears to encompass a significant fraction of asteroids with poorly determined frequency  $s$ .

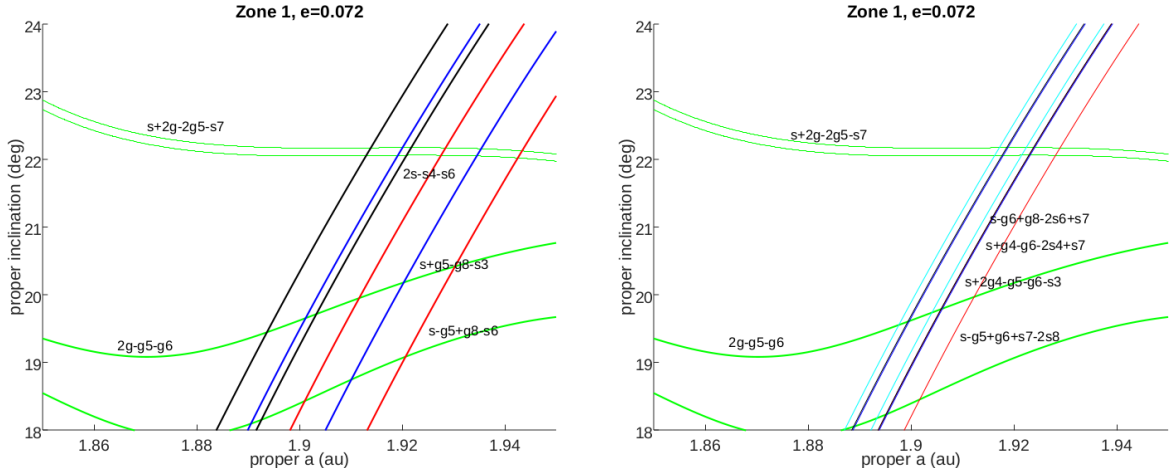


**Fig. 2:** Resonances of  $s$ -type of order 4 (left) and order 6 (right) possibly involved in migratory evolution of orbital inclinations. The resonances of order 4 are plotted with contour lines corresponding to values of the resonant divisor  $(-0.3, 0.3)$  arcsec/yr, these of degree 6 for  $(-0.1, 0.1)$  arcsec/yr. Only the strong  $g$ -type resonance  $2g - g_5 - g_6$  is plotted for divisor values  $(-1, 1)$  arcsec/yr. The pairs of contour lines belonging to the same resonance are of the same color. The resonance positions are computed for  $e=0.072$ .

plausible conclusion is that there is no second family, just the background (unless contradicted when enough physical data become available).

## 2.2. Zone 2

Boundaries of Zone 2 are defined by the mean motion resonances (MMRs)  $4 : 1$  and  $7 : 2$  with Jupiter, thus this zone, excluding narrow regions inside or very near the separatrices of these resonances, covers

a proper semimajor axis range  $2.100 < a < 2.253$  au. The main belt is limited in inclination at its inner boundary due to the presence of a powerful  $g - g_6$  linear secular resonance, thus maximum inclination in the zone does not exceed some 13.5 deg. The eccentricity in the zone is limited by the close encounters with Mars, so that the maximum excentricity for the objects close to the outer boundary of the zone is about 0.25. To be on the safe side, for the fit we

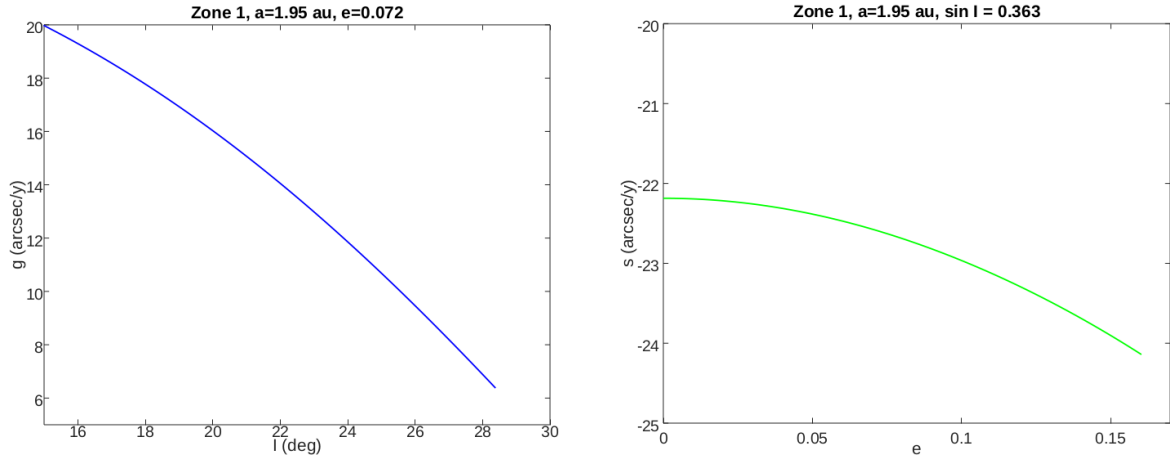


**Fig. 3:** Left: variation of frequency  $g$  as a function of inclination. Right: variation of frequency  $s$  as a function of eccentricity. Note different scales on y-axes. Change of the frequency  $g$  is much larger over the Hungaria region, than that of the frequency  $s$ .

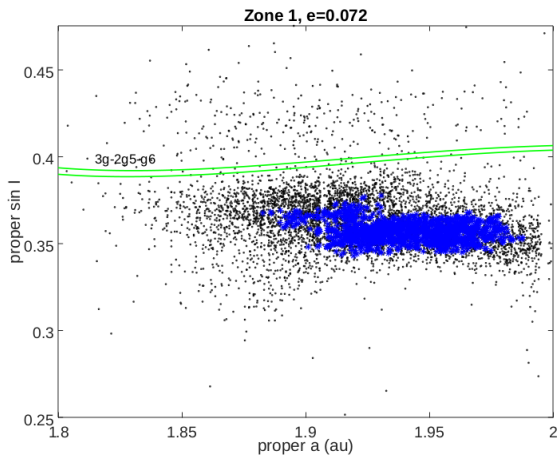


**Fig. 4:** Zone 1 in the proper  $(a, \sin I)$  plane. Black dots: all the asteroids in the zone; blue asterisks: members of the Hungaria family. Position of the secular resonance  $3g - 2g_5 - g_6$  computed for  $e=0.072$ . The resonance delimits the region of the main concentration of Hungaria and the region of the putative second family.

used a total of 16,400 asteroids with  $e_{\max} = 0.20$  and  $I_{\max} = 11$  deg ( $\sin I_{\max} = 0.19$ ). A degree 4 polynomial proved to be sufficient for the fit in this case, consisting of 24 monomials.

The literature on the main asteroid belt is huge and it is not possible to overview it all here. Therefore, for each subsequent zone we shall follow the practice of discussing only the most recent work in connection with the secular resonances and their interaction with local families, leaving to the reader to browse the older references quoted therein.

There are not many families in Zone 2. The most prominent one should be the family of (8) Flora, providing it exists. The controversy regarding the history of its identification and interpretation is de-

scribed in great detail by Knežević (2016) (see also Vokrouhlický et al. (2017a)), who gives an extensive list of relevant references published until 2014. Here we will thus mention only a few more recent papers, including e.g. Nesvorný et al. (2015), and Bolin et al. (2017), who claim that they identified the family, while Oszkiewicz et al. (2015) and Erasmus et al. (2019) warn of a significant diversity in the taxonomy of asteroids in the region. Apart from Flora “family”, only two more families are found in Zone 2: a somewhat dubious (see e.g. Spoto et al. (2015), Milani et al. (2017)) medium-size family of (883) Matteredania (Milani et al. 2014), and the very young family of (1279) Datura (Vokrouhlický et al. 2017b). Neither of them, however, seems to interact with neighboring secular resonances (Carruba et al. 2018).

As seen from Table 2, the overall accuracy of the fit is good, and after removal of outliers it becomes even very good. Both frequencies are in this case fitted with about the same accuracy, indicating that no significant  $g$ -type or  $s$ -type secular resonances dominate the dynamics in the zone. A number of outliers is higher than in Zone 1, but this is easy to explain. From Fig. 5 (top panels), where problematic cases in computation of frequency  $g$  are shown, one can appreciate that majority of the  $3\sigma$  outliers are aligned along the two MMR strips:  $3 : 5$  with Mars at  $\sim 2.142$  au, possibly overlapping with  $1A - 4J + 3N$  ( $A$  - asteroid,  $J$  - Jupiter,  $N$  - Neptune) three-body MMR, and  $4 : 7$  with Mars at  $\sim 2.213$  au, surrounded by neighboring three-body  $7A - 1V - 6J$ ,  $1A - 2J - 4S$ , and  $1A - 4J + 1S$  ( $V$  - Venus,  $S$  - Saturn)<sup>3</sup> ones. In the proper  $(a, e)$  plane (right panel) the red filaments protrude from the region occupied by the bulk of asteroids indicating chaotic drift along the resonance, leakage from the region and possible removal

<sup>3</sup><http://www.fisica.edu.uy/~gallardo/atlas/>, see Gallardo (2014)

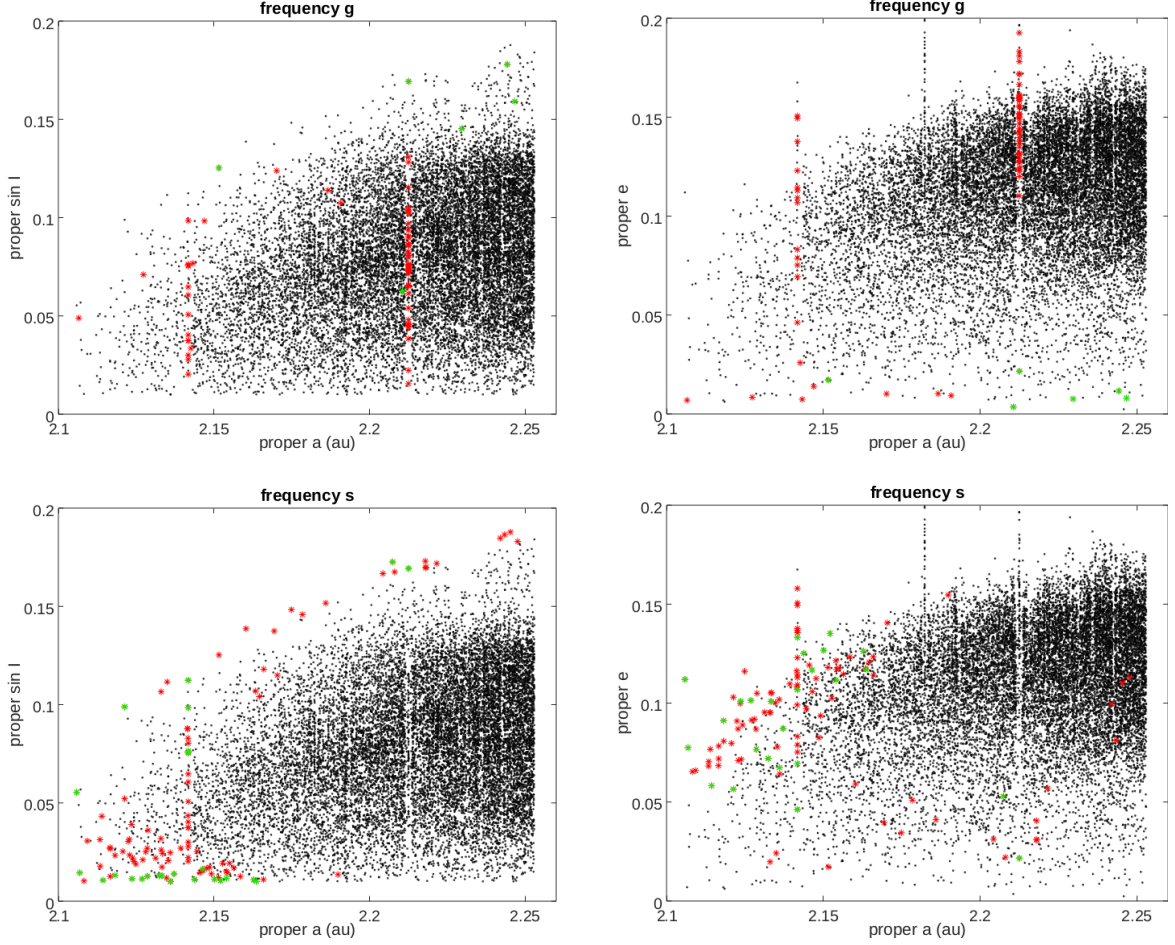


**Fig. 5:** Zone 2 in proper  $(a, \sin I)$  (left) and proper  $(a, e)$  planes: frequency  $g$  (top) and frequency  $s$  (bottom): Black dots: all asteroids in the zone used in the fit; red asterisks: asteroids with absolute values of residuals larger than  $3\sigma$ ; green asterisks: asteroids with absolute values of residuals larger than  $10\sigma$ . Protruding filaments of objects in the right hand side panels indicate leakage of asteroids from the zone.

**Table 2:** The same as in Table 1, but for Zone 2. A total of 16,400 asteroids were used in the fit in this case.

Freq.	$\sigma_{\text{all}}$	$N_{10}$	$\sigma_{10}$	$N_3$	$\sigma_3$
$g$	0.1168	6	0.0433	69	0.0299
$s$	0.0735	25	0.0414	110	0.0321

due to close encounters with Mars. A similar filament of black dots demonstrates that being locked in a weak MMR does not necessarily imply strong chaos nor large proper semimajor axis errors. Several other outliers and all the pathological cases are found at low eccentricities and at high inclinations, close to the bounding secular resonance, which is a typical situation in which cycle slips occur giving rise to erroneous determination of frequencies (Knežević 2020).

In Fig. 5 (bottom panels), where results for frequency  $s$  are shown, one can, however, see a some-

what different picture. There is still alignment of problematic cases along the  $3 : 5$  MMR with Mars, but not along the  $4 : 7$  with Mars one; obviously, the latter resonance in computation of  $s$  produces comparatively smaller effects than in computation of  $g$ , which are masked in computation of standard deviations by the larger effects due to other reasons. These other reasons can be identified by inspecting the bottom part of Fig. 5: most of the outliers and pathological cases in the left panel are either concentrated at very low inclinations (pathological cases being systematically lower than the outliers) or distributed along the border of the strong  $g - g_6$  resonance, while in the right panel these same objects are either having comparatively large, Mars-approaching, or moderate eccentricities, respectively. These observations indicate that the inaccurately determined frequencies in this region are probably due to a combination of the close approaches to Mars, secular resonance effects and cycle slips.

The list of resonances we checked for the presence in the zone contains all the resonances of order 2 and 4 (these corresponding to terms in the disturbing function of degree 2 and 4 in the eccentricity and/or sine of inclination) with Jupiter and Saturn, as well as some resonances of orders 6 and 8, including these with other planets only when necessary. For a complete list of small divisors up to degree 4 appearing in the analytical theory see Table 3.1 in Milani and Knežević (1990); note however, that throughout the zone frequencies,  $g$  are always positive and  $s$  negative within the above defined boundaries of the zone, thus, 17 out of 28 secular divisors actually cannot give rise to resonances. In fact, 10 out of these 17 divisors can give rise to resonances only if the frequency  $g$  becomes negative, which occurs for the inclinations above the boundary of our Zone 2 (in practice, above the  $g - g_5$  resonance, see Fig. 4 in Knežević (2020)). The complete list of relevant resonances in this case consists of only 3 order two (linear) resonances, and 8 order four (nonlinear) ones.

Not even all of these possible resonances were, however, found in the zone. In Fig. 6 the positions of the secular resonances crossing Zone 2, computed for the median proper eccentricity  $e = 0.115$  of the asteroids used in the fit, are shown against the asteroids residing in the zone. They are: the powerful linear resonance  $g - g_6$  bounding the local asteroid population, represented with three contour lines (given with black color) and corresponding to values of the divisor of  $(-1, 0, 1)$  arcsec/yr, the order 6 resonance  $z_2 = 2g - 2g_6 + s - s_6$  and the order 8 resonance  $z_3 = 3g - 3g_6 + s - s_6$ , represented with  $(-0.3, 0.3)$  and  $(-0.1, 0.1)$  arcsec/yr contours (magenta), respectively, crossing the populated parts of the region and belonging to the sequence  $z_k = k(g - g_6) + s - s_6$ , identified and studied by Milani and Knežević (1994). An additional group of 4 resonances: order 4 (blue)  $g - g_5 + s - s_6$ , and order 6 and 8 (green)  $2g - 2g_6 - s + s_6$ ,  $2g - g_5 - g_6 + s - s_6$ ,  $3g - 3g_6 - s + s_6$ , appears in the upper left corner of the plot, but they are of no significance here since they do not cross the region populated with asteroids.

Only the  $z_2$  resonance does cross the Matteredania family and, in the region of crossing, an increased spread of asteroids towards higher inclinations can be noticed, which is probably due to the resonance effect similar to the one discussed above with Hungaria and Hoffmeister families.

### 2.3. Zone 3

Zone 3 stretches over the interval  $2.257 < a < 2.465$  au, hence between the 7 : 2 and 3 : 1 MMRs with Jupiter. Together with Zone 2, it forms the so-called inner asteroid main belt. In terms of eccentricity Zone 2 is still limited from above ( $e_{\max} = 0.30$ ) to avoid unstable asteroids having close approaches to Mars, but in terms of inclination the upper bound is pushed to about 27 deg ( $\sin I_{\max} = 0.45$ ), so that the entire high inclination Phocaea region is included.

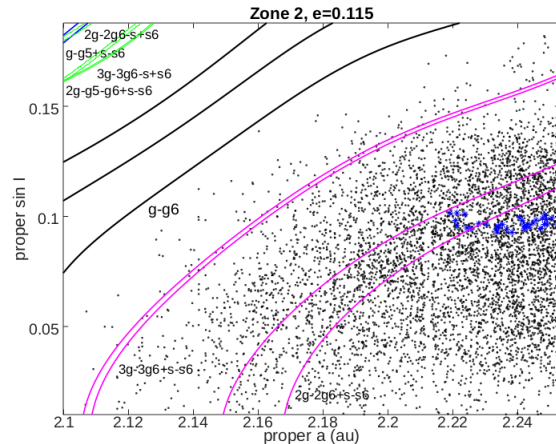


**Fig. 6:** Zone 2 in the proper ( $a, \sin I$ ) plane. Black dots: the asteroids in the zone (only a third is shown in order not to overcrowd the plot); blue asterisks: members of the Matteredania family. Positions of all linear and order 4, as well as of selected order 6 and order 8, nonlinear secular resonances crossing the zone are shown, computed for the median proper eccentricity  $e = 0.115$ .

With a total of 91,772 asteroids, a degree 6 polynomial with 40 terms was used in the fit.

There is a plethora of families in Zone 3, some of which are among the largest and most prominent ones in the entire belt. According to Milani et al. (2014), such are Hertha, Vesta, Massalia and Levin dynamical families, all having complex collisional and dynamical history. Somewhat smaller, but not less interesting, are Phocaea, Erigone, Martes, Sulamitis, Clarissa, Baptistina and Duponta, while still smaller potential families, like Lottie, Philnicholson, and others, are waiting to be fully confirmed or discarded by the new data or perhaps merged with other families with which they have intersections.

Following the rule introduced above, we shall mention just a few recent papers that are important from the point of view of this review. Let us first mention a comprehensive study of Carruba et al. (2016a), who investigated the interaction of the  $z_2$  resonance with the Erigone asteroid family, finding that some 15% of the family members currently librate in that resonance. They also state that slightly less than 5% of members librate in other two order 6 resonances  $2g + g_5 - 3g_6$  and  $g - g_5 + 2s - 2s_6$ .<sup>4</sup> The same family has also been studied by Milani et al. (2019), but in this study focus was on understanding the asymmetric shape of the family (merged with the dynamical family of (5026) Martes) in the phase space of proper elements, in particular the effect of the  $z_2$  resonance giving rise to the asymmetry of velocity distribution.

<sup>4</sup>Carruba et al. (2005) identified 28 order 4 and 6 resonances which cross the inner asteroid belt and involve perturbing planets from Mars to Uranus. Out of these, only  $s - s_6 - g_5 + g_6$  is of interest to us here, and is already included in the analysis.

Milani et al. (2017) analyzed 6 families in more or less strong interaction with secular resonances, searching for the effects such interactions may produce in terms of the shape of the family in the proper elements space, and/or in the family age determination. Out of these only Phocaea family is located in Zone 3, residing in a high inclination Phocaea region, a region long known to be separated from the rest of the asteroid population by strong mean motion and secular resonances. According to this study, about a third of the family members are affected by the  $z_1 = g - g_6 + s - s_6$  resonance, with the values of the divisor within  $\pm 0.5$  arcsec/yr.

Huaman et al. (2018), extending the search for asteroids librating in the  $g - g_6$  linear secular resonance, found that 54% of members of the newly proposed family of (329) Svea, located in Zone 3, exhibit anti-aligned libration in this resonance, as well as a single member of another such new family of (1892) Lucienne.

Although the secular resonances with massive asteroids are not of primary importance in our analysis, let us mention here that, according to Tsirvoulis and Novaković (2016), the Zone 3 families Vesta, Hertha, Erigone, and Levin, interact with either pericentric or nodal linear secular resonance with Vesta.

In Table 3 data illustrating goodness of the fit for Zone 3 are given, which indicate that the quite good accuracy of the fit has been achieved, although the removal of pathological cases and outliers in case of frequency  $g$ , in spite of a rather high number of discarded cases, did not result in such a significant improvement as in Zone 2. Moreover, even if the number of asteroids used in the fit in Zone 3 is about six times larger than in Zone 2, the number of both, pathological cases and outliers in Zone 3, exceeds the corresponding Zone 2 numbers by a much larger factor. Both these observations can be understood as being due to a more complex dynamical environment in Zone 3 than in Zone 2.

**Table 3:** The same as in 1, but for Zone 3. In this zone the largest number of asteroids 91,772 asteroids were used in the fit.

Freq.	$\sigma_{\text{all}}$	$N_{10}$	$\sigma_{10}$	$N_3$	$\sigma_3$
$g$	0.1217	65	0.0979	1229	0.0678
$s$	0.0874	147	0.0459	611	0.0321

Let us, therefore, look in Fig. 7.<sup>5</sup> The distribution of  $10\sigma$  (green) and  $3\sigma$  (red) outliers clearly reveals the main dynamical mechanisms giving rise to a degraded fit accuracy. In the case of frequency  $g$  (Fig. 7 top panels), we can thus see that a majority

<sup>5</sup>Only 1/3 of the asteroids taken into account for the fit in Zone 3 are shown in the panels, to avoid overcrowding of the plots.

of affected asteroids are found along the three dominant MMRs in the outer part of the zone, that a small fraction of asteroids are affected by a few less important MMRs in the inner part, that there exists a problematic high inclination - low eccentricity population, scattered over the entire semimajor axis range, and a couple of groups with rather high sine of inclination ( $\sim 0.3$ ), affected by the secular resonances.

The three dominant MMRs are: the three-body resonance  $1A - 4J + 2S$  at  $a = 2.397$  au, the 1 : 2 resonance with Mars at  $a = 2.419$  au, and the powerful 3 : 1 resonance with Jupiter at  $a = 2.500$  au. The most important argument of the three-body resonance is obviously  $\lambda - 4\lambda_5 + 2\lambda_6 + \varpi$  ( $\lambda, \lambda_5, \lambda_6$  are the orbital longitudes of the asteroid, Jupiter and Saturn, respectively, and  $\varpi$  is the longitude of perihelion of the asteroid), which gives rise to a zero degree eccentricity term in the equations of motion, and, although being of higher order in the masses of perturbing planets, strongly affects the frequency  $g$ . For the other two powerful MMRs we can only say that our pre-fit removal of chaotic and large  $\sigma(a)$  asteroids appears not to be restrictive enough. A minor population in the narrow MMRs obviously does not matter too much in terms of the Zone 3 fit accuracy.

The high inclination - low eccentricity population is, as in all other zones, subject to cycle slips, resulting in deteriorated  $g$  frequencies.

Finally, out of the two distinct groups of problematic cases around  $\sin I \sim 0.3$ , the larger one, centered at  $a \simeq 2.44$  au, contains mostly members of the above mentioned Svea family (Huaman et al. 2018), found to be in anti-aligned libration in  $g - g_6$  secular resonance and therefore having their synthetic  $g$  frequencies in error. For the other group, centered at  $a \simeq 2.34$  au we do not have a plausible explanation: it could be, e.g., some yet undiscovered family at high inclination and low eccentricity, or a secular resonance not included in our analysis (see Fig. 8).

A similar analysis holds for the  $s$  frequency as well. The main difference, however, is that in this case relative importance of MMRs and the  $g - g_6$  secular resonance is reversed, so that the majority of affected asteroids are perfectly aligned with the border of the secular resonance, stretching throughout the entire zone. The number of pathological cases and of outliers for frequency  $s$ , shown in 3, when compared with Zone 2 counterparts, are consistent with the six-fold increase of population, while the resulting standard deviations are nearly equal.

Fig. 8 is analogous to Fig. 6, but with several important differences. The median proper eccentricity in Zone 3 amounts to  $e = 0.138$ , and this value was used for a third, fixed coordinate in computation of resonance positions in the  $(a, \sin I)$  plane. For the purpose of having a clear picture of the resonance web, the figure is splitted in two parts showing resonances of order 2 and 4 in the left panel and those of order 6 and 8 in the right panel; also only 10% of

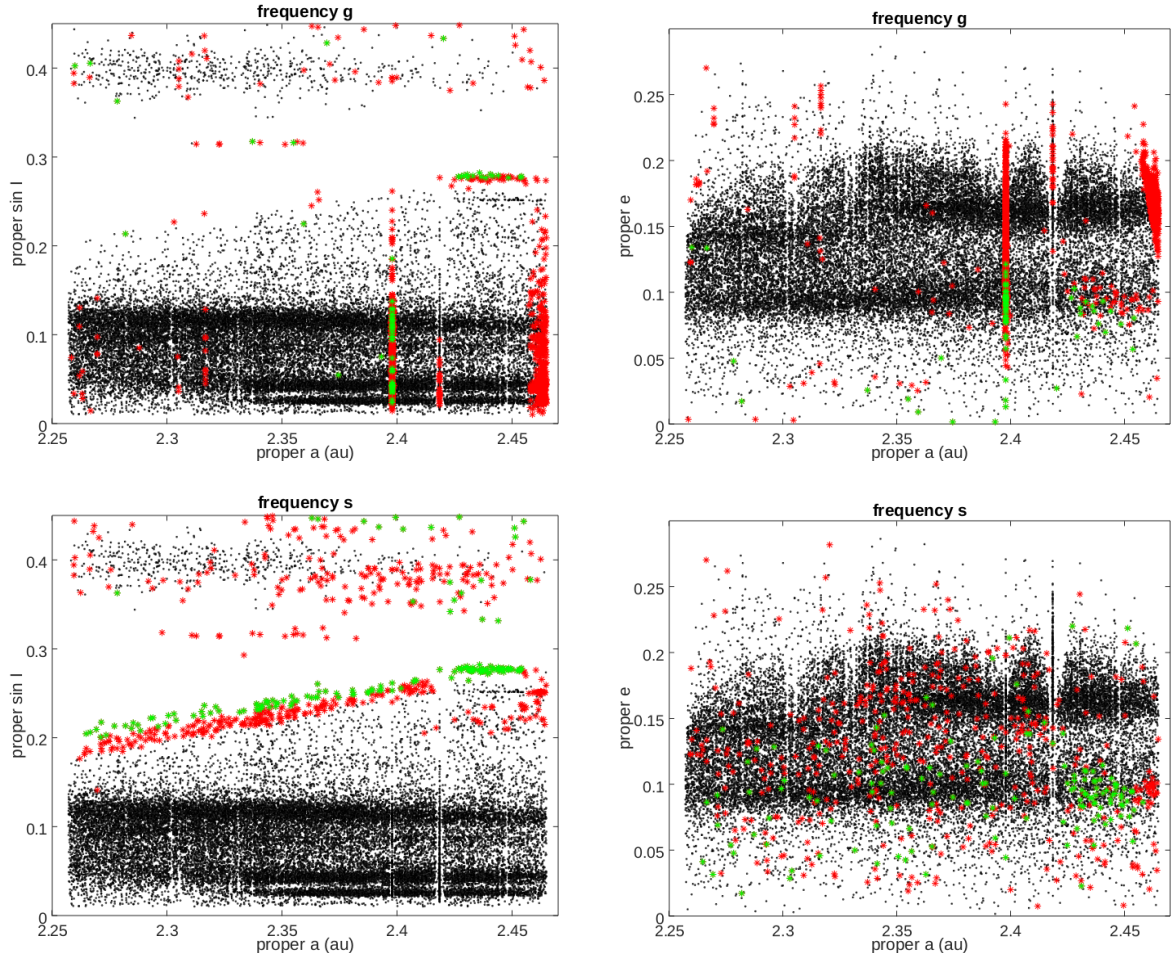


**Fig. 7:** The same as Fig. 5 but for Zone 3. Mean motion resonances, and the edge of the  $g - g_6$  secular resonance are loci of degraded accuracy. Cycle slips affect the high inclination - low eccentricity objects.

all asteroids residing in the zone are plotted as background, against which the resonance contours are superimposed (the same holds for family members).

A fair number of resonances cross Zone 3. The central position is occupied by the powerful linear  $g - g_6$  resonance, bounding the asteroid main belt from above, and separating it from the high inclination Phocaea region. The other linear secular resonance,  $s - s_6$ , shows up in the top left corner of the plot, far from the neighboring asteroid population. Linear resonances are represented with three blue contour lines corresponding to  $(-1, 0, 1)$  arcsec/yr values of the divisor. The three order 4 resonances ( $g - g_6 - s + s_6$ , shown in this zone already by Milani and Knežević (1990),  $2g - g_5 - g_6$ , and  $g - g_5 + s - s_6$ ), represented by the two black contour lines corresponding to  $(-0.5, 0.5)$  arcsec/yr, cut the region at high inclinations. The  $z_2$  and  $z_3$  (magenta), represented by  $(-0.3, 0.3)$  and  $(-0.1, 0.1)$  arcsec/yr contours, respectively, are continuing from Zone 2, with the former one interacting with the Baptistina-Matterania-Levin complex of dynamical families lacking a consistent collisional interpreta-

tion (Milani et al. 2017). Finally, several order 6 ( $2g - g_5 - g_6 - s + s_6$ ,  $2g - g_5 - g_6 + s - s_6$ ,  $2g - 2g_6 - s + s_6$ ) resonances, as well as one order 8 ( $3g - 3g_6 - s + s_6$ ) resonance, all represented with green contour lines corresponding to  $(-0.3, 0.3)$  and  $(-0.1, 0.1)$  arcsec/yr, respectively, complete the list of currently known Zone 3 resonances.

It is, perhaps, worth noticing that the gap between the main belt and Phocaea region seems to be much wider than the region cleared by the sole  $g - g_6$  resonance; actually there are other four (at least) resonances in this void, possibly also contributing to its greater width. Similarly, at least two resonances cross the Phocaea region without giving rise to appreciable effects.

#### 2.4. Zone 4

Zone 4 occupies the region in semimajor axis between  $a = 2.520$  and  $2.701$  au, that is between  $3 : 1$  and  $8 : 3$  MMRs with Jupiter. Hence, with this zone we shift our attention to the central part of the asteroid main belt. The eccentricity is limited to be-

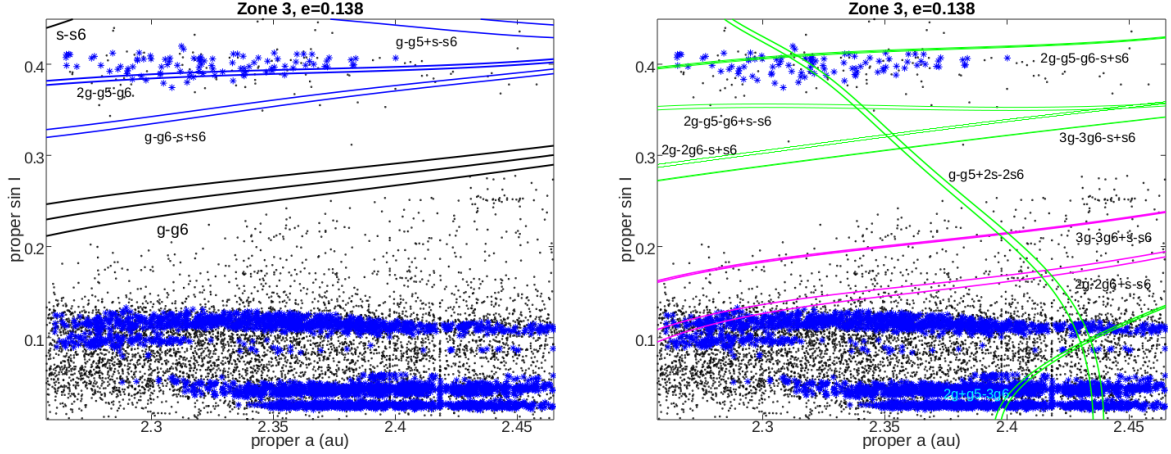


**Fig. 8:** Secular resonances of orders 2 and 4 (left), and of orders 6 and 8 (right). Resonance positions are computed for  $e = 0.138$ . Black dots denote background asteroids, blue asterisks are family members; only a fraction of asteroids are shown in order not to overcrowd the plots. Order 2 (linear) resonances are represented with three black contour lines, the nonlinear resonances of order 4 with two blue lines, order 6 with two green lines, and resonances  $z_2$  and  $z_3$  with two magenta contour lines. The most prominent families are Phocaea ( $\sin I \sim 0.4$ ), Vesta ( $\sin I \sim 0.12$ ), Levin ( $\sin I \sim 0.10$ ), Hertha ( $\sin I \sim 0.04$ ), and Massalia ( $\sin I \sim 0.02$ ).

low  $e_{\max} = 0.30$  and the sine of inclination below  $\sin I_{\max} = 0.55$  ( $I_{\max} \simeq 33$  deg). The zone has already been analysed in Review I (Section 4.3.1), thus we are going to just briefly summarize here the most important findings, and add a few novel results that complement the already published ones.

Due to the presence of the order 4 secular resonance  $g + g_5 - 2g_6$  at low inclinations and the two powerful MMRs bounding the zone, the accuracy of computed frequencies for many asteroids in the zone has been significantly deteriorated. On top of that, there is a comparatively large population of asteroids affected by the cycle slips, so that we had to apply special provisions in this zone. We removed from the fit not only chaotic and large  $\sigma(a)$  asteroids, as in other zones, but in addition we excluded the asteroids with  $\sigma(e) > 0.003$  or  $\sigma(\sin I) > 0.003$ , thus ending up with 87,606 asteroids eligible for the fit. To these we fitted a degree 6 polynomial with 42 monomials (that is, adding terms of degree 4 and 5 in the semimajor axis). These interventions indeed improved the accuracy of the fit, but still the results, in particular those for frequency  $g$ , were among the worst we have got in the entire belt. For the sake of completeness of the present survey, we repeat in Table 4 the information already provided in Review I (Table 4).

**Table 4:** The same as in Table 1, but for Zone 4.

Freq.	$\sigma_{\text{all}}$	$N_{10}$	$\sigma_{10}$	$N_3$	$\sigma_3$
$g$	1.1376	85	0.6795	542	0.5276
$s$	0.1500	85	0.1049	882	0.0724

Even with such comparatively poor results it was, however, possible to identify the main culprits for the deteriorated accuracy, and to determine positions of the selected resonances crossing the zone. The interaction of resonances with families was not discussed, only an apparent overlapping of the  $g - g_5$  resonance with a population of high inclination background objects was briefly mentioned.

The location of the  $g - g_5$  resonance was later studied in great detail in Knežević (2020). It has been found that the accuracy of position of this resonance, which is located in a very high inclination region, can be determined with reasonable accuracy if the polynomial fit is adjusted to local dynamical circumstances, but that a “general” position computed for all asteroids in the zone can be shifted by more than a degree in terms of proper inclination with respect to the “best” position based on the local dynamics.

As for the other recent papers, let us mention (Carruba et al. 2016b), who investigated asteroid families with a leptocurtic distribution of proper inclinations, proposing that such a distribution could be due to the interaction with nodal secular resonances (including the resonances with massive asteroids). Out of eight such families, two high-inclination ones, Hansa and Barcelona, belong to our Zone 4. According to Tsirvoulis and Novaković (2016), Zone 4 families Astraea, Hansa, Barcelona, Maria, Harig and 1986AQ<sub>1</sub> are affected by the resonances with Ceres and Vesta.

In Milani et al. (2017) three families residing in Zone 4 and strongly interacting with secular resonances, were analysed in this respect. For Astraea, with most of the members locked in the  $g + g_5 - 2g_6$

secular resonance, even a special *resonant* proper elements were introduced to better appreciate the true shape and membership of the family. The 2/3 of the members of Barcelona family were found to be strongly affected by the  $g - g_5$  linear secular resonance, with another nonidentified nonlinear resonance mentioned as “relevant for the dynamics of most members”. Only a small fraction of Gersuind family members ( $\sim 14\%$ ) were found to have divisor associated with the  $s - s_6 - g_5 + g_6$  resonance within  $\pm 0.5$  arcsec/yr. In all three cases, however, the effect of the secular resonance to the Yarkovsky drift speed was insignificant, smaller actually than the uncertainty of the Yarkovsky calibration itself.

In [Milani et al. \(2019\)](#), an in-depth analysis of the interaction of a secular resonance  $2g - g_5 - g_6 + s - s_6$  with the Zone 4 family of (480) Hansa indicated crossing of this resonance due to Yarkovsky drift to be responsible for the observed strong asymmetry of the family in terms of proper eccentricity.

Finally, [Pavela et al. \(2021\)](#) investigated effects of the interaction of the Karma asteroid family Yarkovsky migrating members and the local mean motion and secular resonances on the shape of the present day family, characterized by a large scatter of members towards the family edges. They found that the secular resonances  $z_1 = g - g_6 + s - s_6$  and  $s - s_6 - g_5 + g_6$  intersect the family at its inner and outer border, respectively, giving, at least partly, rise to the observed scatter of family members.

[Fig. 9](#) represents a complement to [Fig. 15](#) of [Review I](#), in the sense that it shows only the high inclination region of Zone 4 ( $0.3 < \sin I < 0.55$ ) and gives locations of all the resonances of order 4 and some of degree 6, residing in the region; most of these resonance were not shown in the [Review I](#) figure. Similarly, the families identified by [Milani et al. \(2014\)](#), almost completely missing in the [Review I](#) figure, are represented here with all the known members. Note that Brucato+ label indicates a group of nearby dynamical families: these of (4203) Brucato, (10369) Sinden, (23255) 2000YD<sub>17</sub>, and (116763) 2004EW<sub>7</sub>, for which the collisional origin is not yet fully understood ([Milani et al. 2016](#)). Since computed for the fixed eccentricity  $e = 0.13$  close to the median for all asteroids in the zone and quite different from the values typical of the region ([Knežević 2020](#)), these positions are not very accurate, but they still provide a valuable information on the dense web of resonances in the region.

There is no obvious interaction between the resonances and families in the region. The only feature which can with certainty be attributed to the secular resonance is a gap between Prokne and Hansa families due to the  $g - g_6$  resonance. Possibly that also the “gap” (or rather a lower background density) between Hansa and Brucato families, at about  $\sin I = 0.4$ , can also be considered a consequence of the action of several nonlinear resonances located there.

The secular resonances, on the other hand, significantly affect computation of proper elements. Asteroid proper eccentricities all have  $\sigma(e) > 0.005$  in the high inclination region, including the vicinity of the  $g - g_5$  resonance ([Knežević 2020](#)), as well as in the lower inclination region around the resonance  $g + g_5 - 2g_6$ . Proper inclinations are severely affected along  $s - s_6 - g_5 + g_6$  ( $\sigma(\sin I) > 0.003$ ) and  $z_1 = g - g_6 + s - s_6$  ( $\sigma(\sin I) > 0.005$ ) resonances. On the contrary, the  $g - g_6 - s + s_6$  resonance does not seem to give rise to large errors of proper elements.

## 2.5. Zone 5

Zone 5 is a narrow central belt strip between  $a = 2.708$  and  $2.818$  au, that is between  $8 : 3$  and  $5 : 2$  MMRs with Jupiter. We again limited the eccentricity to  $e_{\max} = 0.30$  and the sine of inclination to  $\sin I_{\max} = 0.55$  ( $I_{\max} \simeq 33$  deg). A total of 56,869 asteroids were used for fitting the frequencies with a 6th degree polynomial comprising 40 terms. No special provisions to improve the accuracy of the fit were needed in this case. An important dynamical property of the zone is the presence of several close MMRs, the three-body  $3J-1S-1A$ , at  $a=2.751$  au, being the most remarkable one.

The large families Agnia (with Jitka), Minerva (Gefion), Hoffmeister, and Dora, the medium size families Merxia, Lydia (Padua), Zdenekhorský, Harig (partly), Astrid, Aeolia, 1992DY<sub>7</sub>, 1995SU<sub>37</sub>, Ino, 1998RH<sub>71</sub>, and Darcydiegel, small but important families like Gallia, Chloris, Watsonia, Tina, Pallas, etc. are all located in this zone.

Several recently published papers deal in one way or another with interaction of secular resonances and asteroid families in Zone 5, thus, we would like to emphasize here some of these results.

Let us first mention the paper by [Carruba and Morbidelli \(2011\)](#), who reported finding an entire asteroid family, that of (1222) Tina, locked in the  $g - g_6$  secular resonance. All the members of the family exhibit an anti-aligned libration of the critical argument, which prevents them from achieving high eccentricities and thus remaining stable for a long period of time. This result was further elaborated in [Carruba et al. \(2018\)](#).

Since (1) Ceres also belongs to Zone 5, the paper by [Novaković et al. \(2015\)](#), in which the effect of the nodal secular resonance with this dwarf planet on the shape of the Hoffmeister family has been demonstrated, deserves to be highlighted here. As authors put it themselves: Ceres’ fingerprint in asteroid dynamics shed light on an entirely new aspect of the long-term asteroid dynamics. This analysis was subsequently extended by [Novaković et al. \(2016\)](#), who revealed the effect of the same mechanism with Astrid family, and by [Tsirvoulis and Novaković \(2016\)](#), who included all linear resonances with Ceres and Vesta in the analysis, and found several families in Zone 5 (e.g. Minerva, Agnia, Chloris, Watsonia, Zdenekhorský) with members in one of these resonances. [Carruba](#)

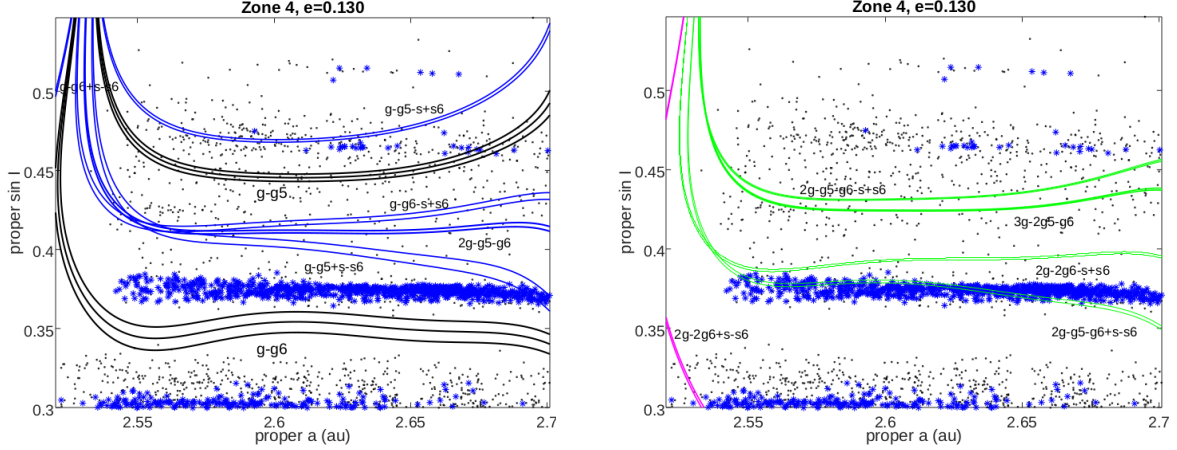


**Fig. 9:** Secular resonances of orders 2 and 4 (left), and of order 6 (right) in the high inclination region of Zone 4. Resonance positions are computed for  $e = 0.130$ . Colors of asteroids and resonant contour lines are as in Fig. 8. The most prominent families in the region are Prokne ( $\sin I \sim 0.3$ ), Hansa ( $\sin I \sim 0.37$ ), Brucato ( $\sin I \sim 0.48$ ), and Barcelona ( $\sin I \sim 0.51$ ).

et al. (2016b) showed that interaction with nodal linear resonance with Vesta significantly alters inclination of a number of members of the Gallia family.

Padua family (formerly named after asteroid (110) Lydia, later proved to be an interloper) is shown already by Milani and Knežević (1992) to be affected by the  $z_1 = g - g_6 + s - s_6$  resonance, and that the long term stability of analytical proper elements of family members has for this reason been seriously deteriorated. Later the  $z_1$  libration state of majority of members was confirmed in a comprehensive study of Carruba (2009), who found that also Agnia family is almost fully emerged in the same resonance, as well as by Milani et al. (2017).

To conclude with references, let us quote another recent paper by Carruba and Barletta (2019) who used the interaction of Yarkovsky migrating family members with nodal linear resonance with Ceres to set up an upper limit to the age of the family.

Summary of the data on the goodness of the fit in Zone 5 is given in Table 5. As one can easily see, the accuracy is comparatively poor, even the best fit  $\sigma_3$  values are barely usable for the accurate determination of secular resonance positions. The difference of the best fit values for the two frequencies is, however, not so large as in Zone 4, the error for frequency  $g$  being smaller and the one for frequency  $s$  larger than the corresponding values in the neighboring zone.

**Table 5:** The same as in Table 1, but for Zone 5. In this zone 56,869 asteroids were used in the fit.

Freq.	$\sigma_{\text{all}}$	$N_{10}$	$\sigma_{10}$	$N_3$	$\sigma_3$
$g$	0.9800	29	0.4915	315	0.3490
$s$	0.3742	91	0.2240	514	0.1371

As shown in Fig. 10 (top panels), the asteroids with poorly determined  $g$  frequency are again mostly found along the border of the powerful 5 : 2 MMR, and in the high inclination - low eccentricity population affected by the cycle slips. An additional concentration at  $\sin I \simeq 0.11$  (top left panel) consists of members of the Harig family, which also have extremely low eccentricities.

The asteroids with poorly determined frequency  $s$ , (Fig. 10, bottom panels), particularly in the  $(a, \sin I)$  plane (bottom left panel) nicely follow the secular resonant contours shown in Fig. 11. One can easily identify slightly tilted strip, extending from about  $\sin I = 0.15$  at the left edge of the plot and stretching along the  $g + g_5 - 2g_6$  resonance, the strongly perturbed group at  $\sin I = 0.35$ , extending along  $g - g_6$  linear resonance and probably affected also by at least three more nonlinear resonances ( $s - s_6 - g_5 + g_6$ ,  $g - g_5 + s - s_6$ ,  $2g - g_5 - g_6 + s - s_6$ ), another similarly aligned concentration at  $\sin I = 0.42$  of objects close to  $g - g_5$  linear resonance, and possibly crossed by the  $g - g_6 - s + s_6$  and  $2g - g_5 - g_6$  order 4 resonances, as well as by some resonances of order 6 and 8. The population above  $\sin I = 0.5$  has so high inclinations that the determination of frequencies is seriously degraded regardless of the low or not low eccentricity and cycle slips.<sup>6</sup>

As shown already by Milani and Knežević (1990), there are only two secular resonances in the low inclination region of Zone 5, but many in the high inclination region (see Fig. 11). Hence, also the interaction between secular resonances and asteroid families is scarce and limited to the high inclination families only.

<sup>6</sup>By using in the polynomial fit only asteroids with  $\sin I < 0.3$  the accuracy of the frequencies would improve by a factor 2 – 3.

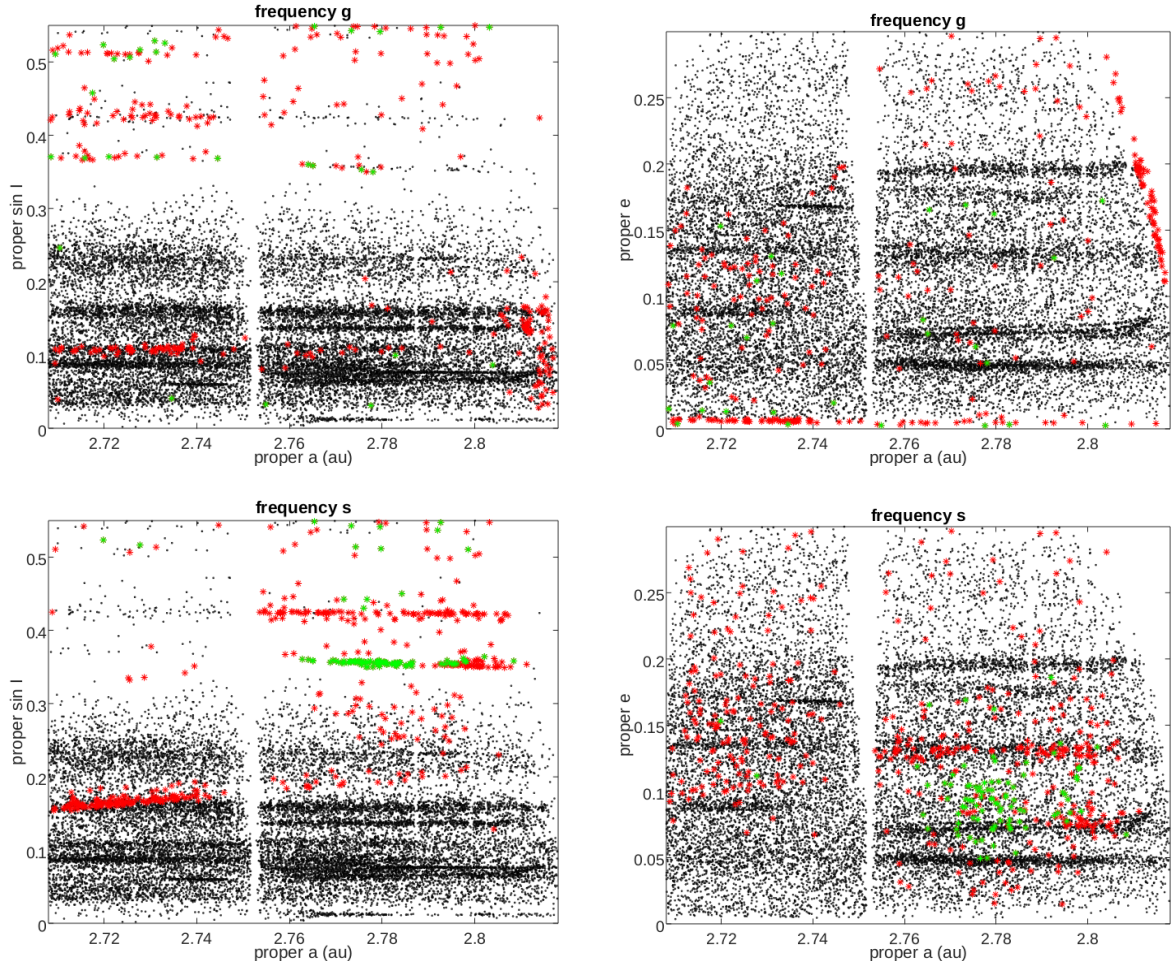


**Fig. 10:** The same as Fig. 5 but for Zone 5. Boundary of the strong mean motion resonance  $5 : 2$  for frequency  $g$  (top panels), and the border of the  $g - g_6$  secular resonance for frequency  $s$  (bottom panels) are loci of degraded accuracy. Cycle slips affect determination of  $g$  for high inclination - low eccentricity objects. The gap at about  $a = 2.751$  au is due to a pre-fit removal of objects affected by a group of nearby MMRs, including the 3J-1S-1A three-body one. Only half of the objects residing in the zone is shown.

Two distinct concentrations of asteroids with a poorly determined frequency  $s$  are distinguishable in the  $(a, e)$  plane (bottom right panel). The strongly affected group (green and red points), scattered in terms of eccentricity ( $0.05 < e < 0.13$ ) corresponds to the above mentioned compact group at  $\sin I = 0.35$ , while the more compact cluster of red points at about  $e = 0.13$  corresponds to the high inclination concentration at  $\sin I = 0.42$ . Both these groups, as already mentioned above, actually represent examples of the interaction of secular resonances with asteroid families: that of (1222) Tina, found to be in the anti-aligned libration in  $g - g_6$ , and (148) Gallia, affected by long term resonant effect by a massive asteroid (4) Vesta, respectively. Let us also mention very high inclination ( $\sin I > 0.5$ ) family of (2) Pallas with a number of members with inaccurate frequencies.

Curiously enough, there exists in Zone 5 a significant population of very low inclination asteroids

belonging to Astrid family (see Fig. 10, left panels), which do not exhibit large errors of frequency  $s$ . In other words, the cycle slips in proper longitude of the node  $\Omega$  do not occur. The explanation for this can be that the eccentricities of these objects are all low to moderate, thus giving rise to comparatively small amplitude secular variations of the proper angle, and to no or seldom occurrence of cycle slips.

## 2.6. Zone 6

Zone 6 in our definition covers the region between  $a = 2.83$  au and  $a = 2.95$  au, or between strong  $5 : 2$  and  $7 : 3$  MMRs with Jupiter, and extends up to  $e_{\max} = 0.30$  and  $\sin I_{\max} = 0.35$  ( $I_{\max} \simeq 20$  deg) in terms of eccentricity and inclination, respectively. A total of 20,094 asteroids were used to fit the frequencies with a 6th degree polynomial comprising 40 terms. No special provisions to improve the accuracy of the fit were needed in this case. Sev-

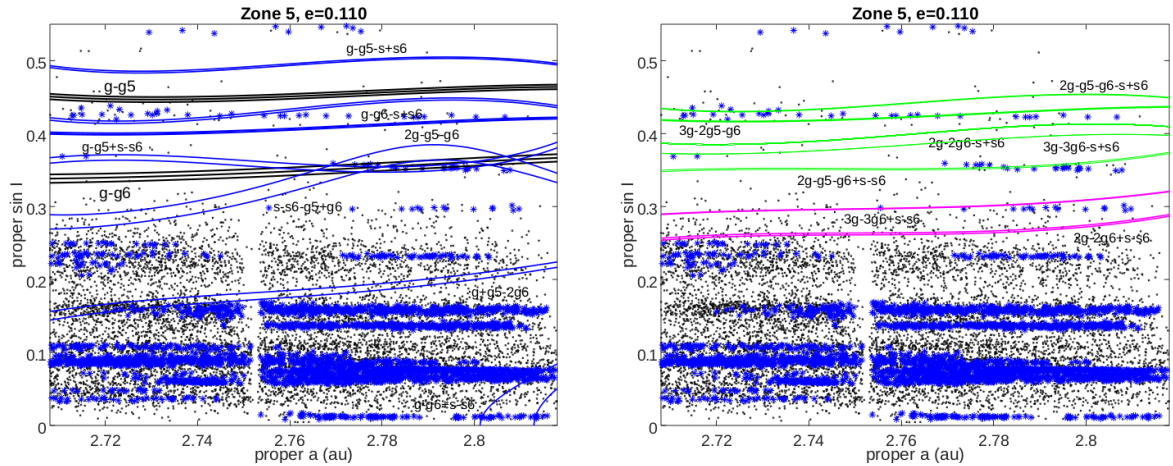


**Fig. 11:** Secular resonances of orders 2 and 4 (left), and of order 6 and 8 (right) in Zone 5. Resonance positions are computed for  $e = 0.11$ . The colors of the asteroids (only a half of which is shown in the plots) and of the resonant contours are the same as in Fig. 8. Families are Pallas ( $\sin I \sim 0.55$ ), Gallia ( $\sin I \sim 0.43$ ), Watsonia ( $\sin I \sim 0.30$ ), Eunomia ( $\sin I \sim 0.23$ ), Minerva ( $\sin I \sim 0.16$ ), Dora ( $\sin I \sim 0.14$ ), etc.

eral closely packed three-body MMRs are present in the zone:  $2J+1S-1A$  at  $a=2.900$  au,  $8J-2S-3A$  at  $a=2.902$  au,  $6J-3S-2A$  at  $a=2.903$  au, and  $10J-7S-3A$  at  $a=2.904$  au, the latter being the most remarkable one. Curiously enough, there seems to be another MMR at  $a = 2.909$  au, which we could not identify in the Atlas of Resonances (Gallardo 2014).

This part of the Main Belt is known for its low number density of asteroids and comparatively few, clearly separated families, with only a single big, old family found there, that of (158) Koronis. Hence, the asteroids in the zone should in a good part be primordial, and the zone is colloquially called “the pristine zone”. According to Brož et al. (2013), these features are due to the fact that the above mentioned strong bounding MMRs prevent asteroids from neighboring zones to enter the zone while migrating due to the Yarkovsky effect, and to the small size of the zone allowing only a few families to be formed. Let us note, however, that Tsirvoulis et al. (2018) found a significant portion of the large Eos family to protrude to the pristine zone from the neighboring Zone 7.

Apart from the big Koronis family, Tsirvoulis et al. (2018) report 15 smaller ones, coming from different classifications, out of which the most important ones are families of (293) Brasilia, (845) Naema, and (1189) Terentia.

Let us begin the overview of the references for Zone 6 with recalling a seminal paper by Bottke et al. (2001), in which the so-called “Prometheus surge” in the Koronis family has been explained as due to the interaction with a secular resonance. The surge consists of a part of the members of Koronis family, located at the high semimajor axis side of the family, which exhibit systematically larger proper eccentricities than the rest of the family (see Fig. 12, panels on the right hand side) as a consequence of the interac-

tion of family members migrating outwards from the Sun due to Yarkovsky effect, with the secular resonance  $g + 2g_5 - 3g_6$ .

Only a handful of recently published papers deal with the Zone 6 families, among which we found only one dealing, to some extent, with secular dynamics of the families. Namely, in their analysis of the Koronis family original velocity field, Carruba et al. (2016c) identified likely resonators (asteroids having the value of the critical divisor within  $\pm 0.3$  arcsec/yr from the resonance center) in two order 6 nonlinear secular resonances: the already mentioned  $g + 2g_5 - 3g_6$  one, with 167 resonant candidates, and  $s - s_6 - 2g_5 + 2g_6$ , located near the outer border of the family, with 42 such objects. Confirming, as regards the former resonance, the results obtained by Bottke et al. (2001) in terms of the eccentricity surge, they also found several asteroids scattered by the latter resonance in terms of the inclination.

Data on the goodness of the fit for Zone 6 are presented in Table 6. As one can appreciate from these data, the accuracy of the fit is much better than in the neighboring Zone 5, especially for frequency  $s$ . For frequency  $g$  the results are also better, but not that much, in particular in comparison with the accuracy of the fit achieved in Zones 2 and 3. This may actually appear as a bit surprising, bearing in mind that the “pristine zone” has always been considered as dynamically quiet (Carruba et al. 2016c), with no major resonances affecting the dynamics. The number of outliers in case of frequency  $g$  is not too big, with also not many “pathological” cases with extremely large residuals. Let us, therefore, inspect the usual plots revealing the locations of outliers and the dynamical mechanisms responsible for the less accurate results.

As in most previous cases, in all the panels of Fig. 12 a remarkable concentrations of the low ac-

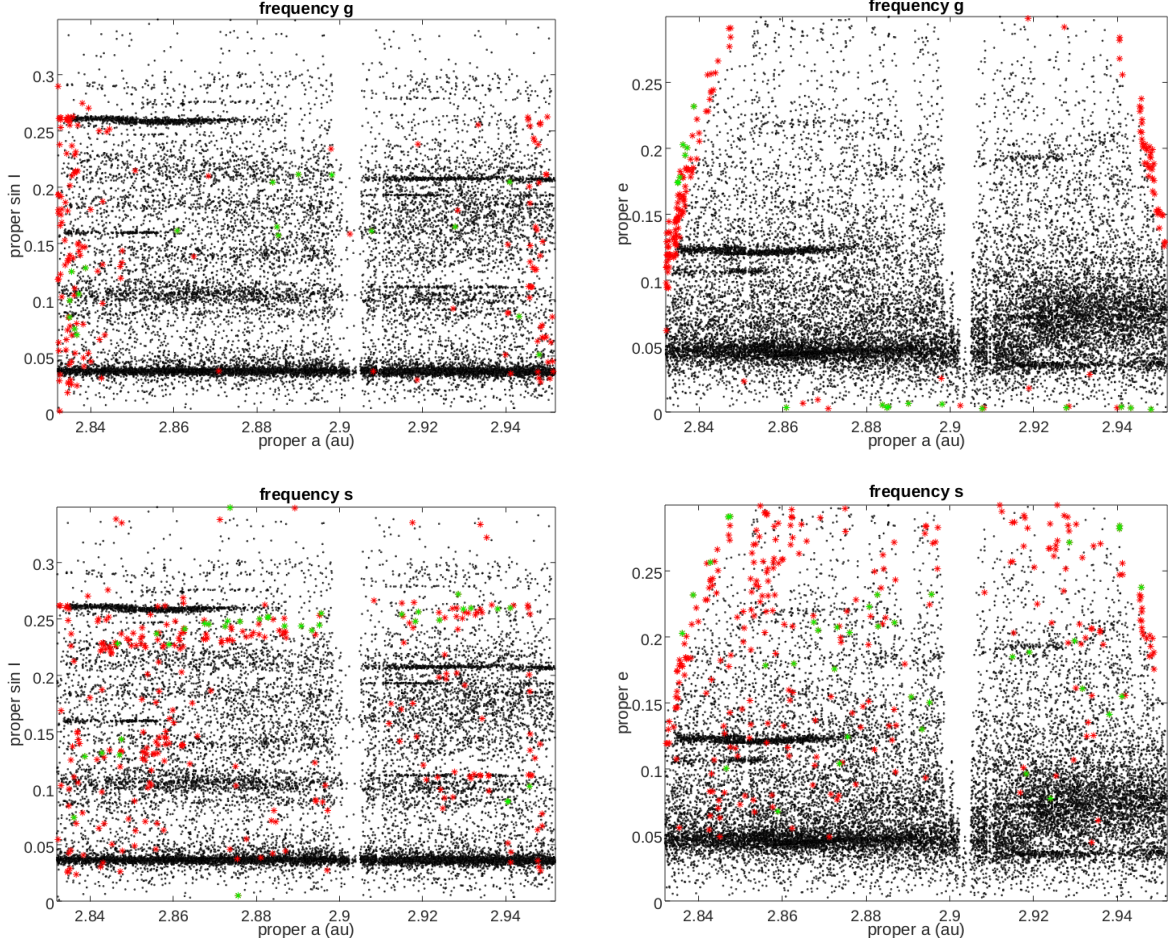


**Fig. 12:** The same as Fig. 5 but for Zone 6. Asteroids with degraded accuracy of frequencies are aligned along the edges of strong mean motion resonances  $5 : 2$  and  $7 : 3$  with Jupiter for frequency  $g$  (top panels), and along the  $g + g_5 - 2g_6$  secular resonance for frequency  $s$  (bottom panels). The gap at about  $a = 2.9$  au is due to a pre-fit removal of objects affected by a group of close MMRs.

**Table 6:** The same as in Table 1, but for Zone 6. In this zone 20,094 asteroids were used in the fit.

Freq.	$\sigma_{\text{all}}$	$N_{10}$	$\sigma_{10}$	$N_3$	$\sigma_3$
$g$	0.4744	18	0.3474	179	0.2644
$s$	0.0620	36	0.0461	305	0.0279

curacy results are found along the edges of the two powerful MMRs marking the borders of the Zone. Obviously, such outcome could have been avoided by relaxing somewhat the pre fit removal criteria and thus widening the resonant region. A gap in the middle of the plots is, on the other hand, an example of successful removal of the affected objects, in this case from the surroundings of the above mentioned group of MMRs, since no asteroids with large residuals appear there. In the case of frequency  $g$  (top panels), slightly peculiar may appear the fact that there are

some pathological cases with low eccentricities, but having only moderately high inclinations. Instead, one can see a clear alignment of asteroids with large residuals in frequency  $s$  along the  $g + g_5 - 2g_6$  resonance (compare the bottom left panel and Fig. 13), which can be understood as due to the fact that these asteroids mostly have quite high eccentricities (bottom right panel) and are, therefore, strongly affected by this resonance.

Only two nonlinear secular resonances are present at moderate inclinations in Zone 6 (Fig. 13, left panel):  $z_1 = g - g_6 + s - s_6$  and  $g + g_5 - 2g_6$ . The  $z_1$  resonance in the region of low semimajor axes, to the left of the central void, interacts with the family of (16286) 4057P-L, while in the region of the higher semimajor axes, to the right of the void, it coincides with a significant number density drop, thus presumably giving rise to the observed gap.

Three more resonances appear at high and very high inclination:  $z_2 = 2g - 2g_6 + s - s_6$ ,  $z_3 = 3g - 3g_6 + s - s_6$ , and  $s - s_6 - g_5 + g_6$ . Neither of them seems

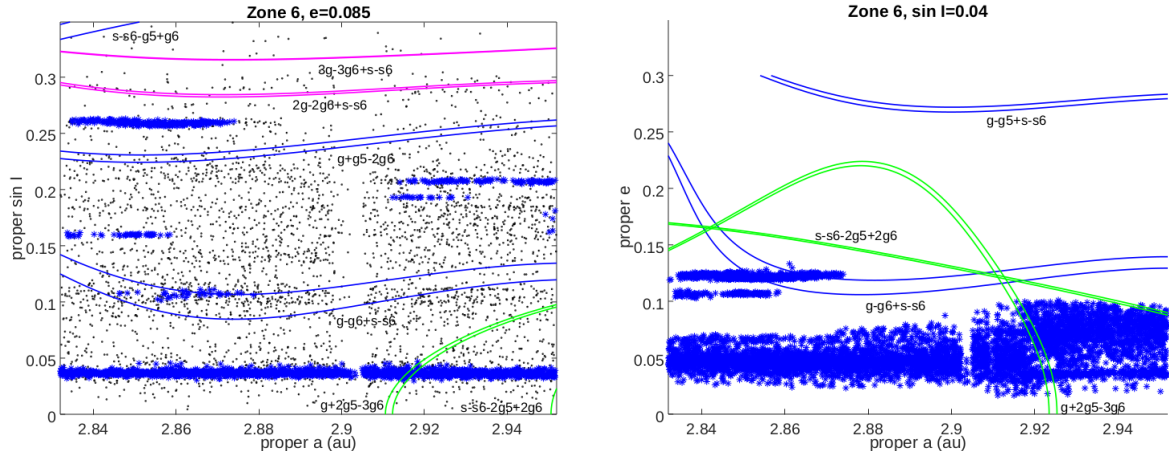


**Fig. 13:** Secular resonances in Zone 6. In the left panel resonances are shown in the  $(a, \sin I)$  plane with positions computed for  $e = 0.085$ ; a third of the objects in the zone are plotted. In the right panel resonances are shown in the  $(a, e)$  plane with positions computed for  $\sin I = 0.04$ , which corresponds to the bulk of Koronis family (in this plot only the asteroids belonging to the families are shown). The colors of the asteroids and of the resonant contours are the same as in Fig. 8. Significant families in the zone are Brasilia ( $\sin I \sim 0.26$ ,  $e \sim 0.12$ ), Naema ( $\sin I \sim 0.21$ ,  $e \sim 0.03$ ), and Koronis ( $\sin I \sim 0.04$ ,  $e \sim 0.05$ ).

to affect visibly the neighboring asteroids. Taking into account the paucity of objects in high inclination region of Zone 6, this could very well be expected.

Finally, of the two resonances mentioned by Caruba et al. (2016c), the  $3g+2g_5-3g_6$  one, as expected, crosses Koronis family, while the  $s-s_6-2g_5+2g_6$  one appears only partly in the lower right angle being almost all out of the plot; one can conjecture that it is so close to the  $7:3$  MMR that its position could not be very accurately determined.

As already mentioned above in the review of the literature, this zone is special in the sense that it hosts the well known example of the interaction of the migrating Koronis family members and the  $g+2g_5-3g_6$  resonance, giving rise to the Prometheus surge. Therefore, in the right panel of Fig. 13 we plotted the secular resonances in the  $(a, e)$  plane to emphasize the fact that the resonance indeed delineate the two parts of the family with different dynamical evolution. The position is given for the value of the fixed inclination  $\sin I = 0.04$ , closely corresponding to the bulk of the Koronis family members. Also, for clarity, no background asteroids are plotted in this case.

## 2.7. Zone 7

Zone 7 spans the region between  $a = 2.956$  au and  $a = 3.07$  au, that is between  $7:3$  and  $11:5$  MMRs with Jupiter. In our definition it also extends up to  $e_{\max} = 0.30$  in eccentricity, and up to  $\sin I_{\max} = 0.35$  ( $I_{\max} \simeq 20$  deg) in inclination. In the frequency fit we used 36,619 asteroids, while the 4th degree polynomial with 20 terms was considered as sufficient in this case. The dominant dynamical feature of the zone is the presence of the  $9:4$  MMR at about 3.03 au

leaving a rather large void in the middle of the zone after the pre fit removal of asteroids with deteriorated catalog frequencies.

The largest family extending over the entire zone is Eos family. It is accompanied with medium size Emma and Klytaemnestra, and small size Aegle, Anfimov, Inarradas families. No tiny candidate families were identified in this zone.

Quite naturally, Eos family received the largest attention of researchers in the past. Many studies were published dealing with various aspects of determination of its membership, the dynamical and physical properties of its members, as well as with its origin and dynamical and collisional evolution. However, when the interaction of family members with secular resonances is in question, the studies are not so numerous.

In the classical papers by Milani and Knežević (1990, 1992), it has been shown that the nearby non-linear secular resonances  $z_1 = g - g_6 + s - s_6$  and  $g - g_5 + s - s_7$ , the latter involving also Uranus, intersect the Eos family and affect the accuracy of computation of proper elements of the family members. The asteroid (221) Eos itself, and a number of other family members were found to be in libration in  $z_1$ , but this apparently did not deteriorate the proper elements to the point that these asteroids could not be recognized as being members of the family.

The interaction of Eos family with  $z_1$  resonance is also investigated by Vokrouhlický et al. (2006) who found that this interaction is amplified when Yarkovsky forces are taken into account. If captured in the resonance for long enough time, asteroids' orbital elements "slide" along the resonance while bodies migrate in terms of the semimajor axis, which explains some peculiarities of the family structure.

A gap in the  $(a, \sin I)$  projection for low values of  $a$ , which opens between the two parts of the family of (283) Emma, is interpreted by Milani et al. (2017) as due to the  $z_1$  resonance crossing the family. According to these authors, about 8% of the family members are affected by this resonance, but not also the corresponding IN side of the family V-shape. They classify the family as of cratering type with a visible double jet shape. In the same paper, they already speculate about possible contamination of the Klytaemnestra family with interlopers from the nearby large Eos family, transported from the latter to the former via the  $z_1$  secular resonance (see e.g. Vokrouhlický and Brož (2002), Carruba et al. (2014b)) for demonstration of such transport).

The problem of Klytaemnestra family has been thoroughly studied in another paper by Milani et al. (2019) who state that this is a significant dynamical family with more than 500 members, which, however, lacks the collisional interpretation. To solve the puzzle, they propose to split the family into three parts: a small cratering cluster around (197) Klytaemnestra, a bigger fragmentation one surrounding the (9506) Telramund, plus "a bridge" of Eos family interlopers transported there by the  $z_1$  resonance and giving rise to the chaining effect, artificially joining the two originally separate clusters together.

Finally, the group of (633) Zelima, a sub-family of the large Eos family, has recently been identified by Tsirvoulis (2019), who also noticed that the whole cluster seem to be "born" inside the  $z_1$  secular resonance since all the members of the cluster exhibit a large amplitude libration of the  $\sigma = \varpi - \varpi_6 + \Omega - \Omega_6$  critical argument and corresponding oscillations of proper eccentricities and inclinations. That all the members of the cluster indeed librate in this resonance was subsequently confirmed by Carruba and Ribeiro (2020), who used this unique feature of the family to infer its age using a method based on the dispersion of members in the  $(\sigma, \dot{\sigma})$  plane.

Table 7 shows data on the goodness of the fit for Zone 7. The numbers for frequency  $g$  are similar or slightly better than in the neighboring Zone 6. For frequency  $s$ , however, they are not so good, and actually rather similar to those for Zone 4, including a very large number of the  $3\sigma$  outliers.

**Table 7:** The same as in Table 1, but for Zone 7. 36,619 asteroids were used in the fit.

Freq.	$\sigma_{\text{all}}$	$N_{10}$	$\sigma_{10}$	$N_3$	$\sigma_3$
$g$	0.5627	19	0.2176	76	0.1997
$s$	0.1502	32	0.1399	784	0.0907

When speaking of the dynamical mechanisms responsible for the computation of frequencies with deteriorated accuracy, in case of frequency  $g$  these are for the most part the same as in all previous

zones: the MMR resonances where the fit outliers align along the resonant borders, here primarily at the edge of the 7 : 3 resonance with Jupiter marking the inner boundary of Zone 7, and extremely small proper eccentricities combined with moderately high inclinations indicating possible problems with cycle slips. The situation is less clear with frequency  $s$ , where numerous outliers are spread out throughout the entire zone. The largest concentration is observed at high eccentricities, while the distribution in terms of inclination exhibits three different regions (at  $\sin I \simeq 0.03, 0.18, 0.30$ ) of increased presence, some of which can perhaps be associated with secular resonances (see Fig. 15), but most cannot. One possibility could be the insufficiently accurate polynomial fit, because in this zone only monomials up to degree 4 were taken into account.

The web of secular resonances present in Zone 7 exhibits two interesting components. One is the usual bunch of different weak resonances crossing the zone at high inclination, but here also including the  $g + g_5 - 2g_6$  resonance, quite important in lower inclination regions in previously examined zones, which now rises into much higher (and less populated) regions. The other pertains to the fact that beyond 3 au, the  $z_1$  resonance overlaps with two order 6 secular resonances, the  $g + 2g_5 - 3g_6$  and  $s - s_6 + 2g_5 - 2g_6$ , which certainly contribute to the interaction of the whole set with the Eos family.

## 2.8. Zone 8

Zone 8 comprises the region between  $a = 3.08$  au and  $a = 3.172$  au, that is between 11 : 5 two-body and  $5J - 2S - 2A$  three-body MMRs with Jupiter and with Jupiter and Saturn, respectively. In eccentricity it extends up to moderate  $e_{\text{max}} = 0.30$ , but up to as much as  $\sin I_{\text{max}} = 0.48$  ( $I_{\text{max}} = 29$  deg) in inclination (in order to include the high inclination family of (31) Euphrosyne). For the fit 38,520 asteroids were used in this case, as well as the 6th degree polynomial with 40 terms. The most prominent MMRs inside the zone are 13 : 6 at 3.106 au, and the associated sequence of 15 : 7, 17 : 8, 19 : 9, ... ones gradually approaching the outer edge of the zone. In our representation (see Fig. 16) all of them are associated with visible gaps due to the pre fit removal of asteroids with inaccurate catalog frequencies.

A couple of particular features of Zone 8 are connected with the families. The first one pertains to an extraordinarily large number of families in such a comparatively small zone, witnessing of the intense collisional evolution of the far outer part of the asteroid main belt: at least 27 families are completely or at least partly present inside it (Milani et al. 2014). The other one regards its outer border coinciding with the powerful three-body mean motion resonance (Nesvorný and Morbidelli 1998), which, unlike the most of the MMRs bordering other zones, was not strong enough to act as a barrier preventing the "spill-over" of the families to the neighboring Zone 9.

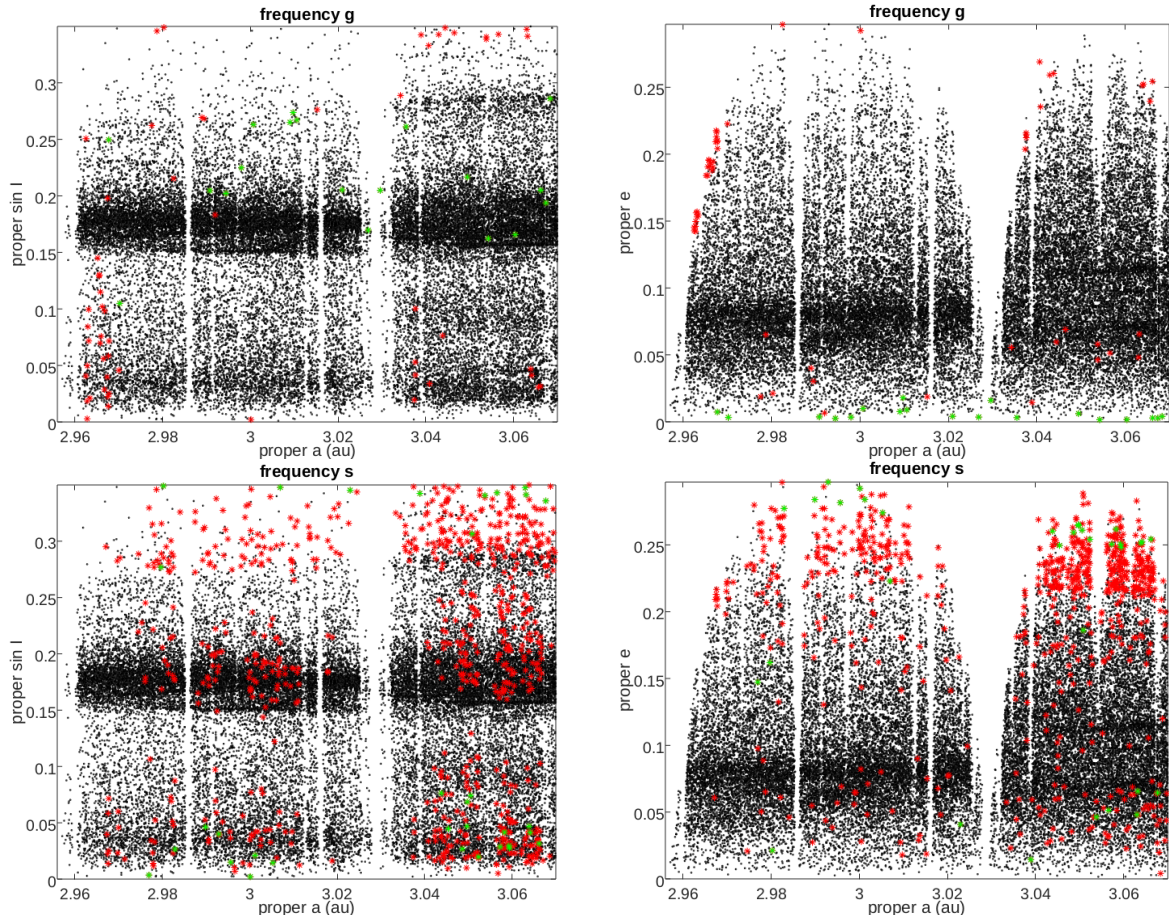


**Fig. 14:** The same as Fig. 5 but for Zone 7. The gap at about  $a = 3.05$  au is due to a pre-fit removal of objects affected by the strong  $9 : 4$  MMR with Jupiter.

Three large (Themis, Hygiea, Veritas), and some of the several medium (Euphrosyne, Gantrisch, Ursula, Struveana, Laodica, Nocturna) families actually extend on both sides of this boundary making it less dynamically justified than in other cases. Large family Klumpkea is entirely contained in Zone 8; in addition, there are 8 small and 4 tiny families in this zone.

Families in Zone 8 were extensively studied in the past, due to their strong interaction with various resonances. Among the comparatively recent studies the interaction of the high inclination Euphrosyne family with secular resonances, in particular with the strong  $g - g_6$  linear secular resonance crossing the core of the family, attracted a special attention. Thus, [Machuca and Carruba \(2012\)](#) draw attention to the fact that the region in which the Euphrosyne family resides is crossed by several secular resonances, both linear and non linear, and that a fair number of asteroids in the region exhibit either aligned or anti-aligned libration in one of these resonances, or switch between libration and circulation. Repeating the same exercise, [Carruba et al. \(2014a\)](#) confirmed that a significant

number of family members indeed is in anti-aligned libration in the  $g - g_6$  resonance, and proposed that the steep size distribution of the Euphrosyne family can be explained by this fact. [Masiero et al. \(2015\)](#) studied the possible contribution of the Euphrosyne family to the low albedo Near-Earth asteroids. They claim that 1% of the current population likely originated as family members, becoming NEAs by slow pumping of the eccentricity due to resonances (presumably also to  $g - g_6$ ). [Tsirvoulis and Novaković \(2016\)](#) found that Euphrosyne family is crossed by the linear secular resonances with (1) Ceres and (4) Vesta, hinting at possible interaction between the crossing resonances which may amplify the resonant effects in the post-formation evolution.

A thorough analysis of the collisional model compatible with the observed dynamical features of the Euphrosyne family has been made by [Milani et al. \(2019\)](#). They addressed several issues: combining the initial velocity field and spin they assessed the post-impact dynamical evolution of the family members which migrate into the  $g - g_6$  secular resonance

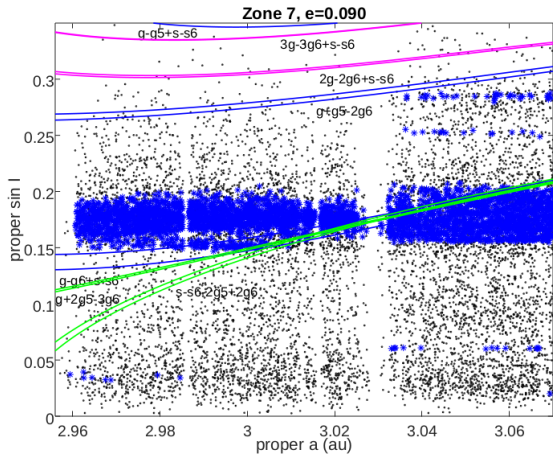


**Fig. 15:** Secular resonances in Zone 7. Resonance positions are computed for  $e = 0.09$ . The colors of the asteroids (only one third of which is shown in the plot) and of the resonant contours are the same as in Fig. 8. The dominant family in the plot is Eos with Klytaemnestra nearly attached to it at  $a < 3.015$  au and  $\sin I \sim 0.15$ .

due to the Yarkovsky effect, possibly also encounter the  $5J - 2S - 2A$  three-body mean motion resonance, and often end up in the hyperbolic orbits; allowing for the fact that a quantitative estimate of this loss of objects may be too complex, they conclude that the family “must have been much larger than it is today, with the majority of the original members now being interstellar”. Assuming a single collision origin, they speculate that the asymmetry in terms of proper eccentricity on the two sides of the  $g - g_6$  resonance could be due to a selection effect. Finally, they also consider the possibility of existence of two families of different age, admitting that there is no sufficient evidence to prefer either this or a single family solution.

Let us conclude this brief overview of the recent literature on the interaction of secular resonances and asteroid families in Zone 8 with the paper by Carruba et al. (2014b) who analyzed the dynamics of members of the Hygiea family in presence of secular resonances finding asteroids in librating states in the  $z_1 = g - g_6 + s - s_6$ ,  $g + 2g_5 - 3g_6$ , and  $s - s_6 - 2g_5 + 2g_6$  resonances, with only a few temporary librators found in the  $g - g_5 + 2s - 2s_6$  one.

When frequency  $g$  is in question, the goodness of the fit test showed very poor results (actually the worst of all the Zones) when all the asteroids in the Zone 8 are taken into account, but removal of a comparatively small number of outliers with extreme and large residuals gives results not very different from those in the neighboring Zone 7. This indicates that in this zone there exists a handful of “pathological” objects with really large residuals, but that overall accuracy of the fit can be considered satisfactory. The fit of frequency  $s$  is again much better, in particular after removal of the outliers, and comparable with the accuracy of the fit in most of the other zones.

There is little new to say about the distribution in the space of proper elements of asteroids for which the frequencies are determined with low accuracy (see Fig. 16). In the case of frequency  $g$  (top panels) most of the outliers are located at very high inclination, with the largest number of such objects aligned along the  $g - g_6$  resonance (Fig. 17), hence mainly in the Euphrosyne family. Several “pathological” cases, located at the extremely low eccentricities, are again presumably due to the cycle slips. Basically the same can be said for the frequency  $s$ , with the only difference that the number of outliers is higher in this case (see Table 8), and that there are no objects affected by the cycle slips. A group of outliers at the inner boundary of the zone (along the  $11 : 5$  MMR with Jupiter) probably belongs to the Euphrosyne family’s tail which ends up in this powerful resonance.

**Table 8:** The same as in Table 1, but for Zone 8. 38,520 asteroids were used in the fit.

Freq.	$\sigma_{\text{all}}$	$N_{10}$	$\sigma_{10}$	$N_3$	$\sigma_3$
$g$	1.3673	20	0.3353	52	0.2720
$s$	0.2237	33	0.1235	243	0.1000

We were able to identify as many as 15 secular resonances of different orders in the high inclination region of Zone 8, but none below  $\sin I = 0.20$ . Therefore, in Fig. 17 only this region containing the resonance locations is shown.

The most important resonance present in the zone is obviously the  $g - g_6$  one, for which we observe an alignment of asteroids with large residuals of both proper frequencies, and which hosts a number of librators mentioned in the literature. The fit may seem not to be very precise (the resonance contours appear a bit low with respect to the positions of outliers), but if one computes the position of the resonance for the fixed eccentricity of  $e = 0.14$ , which corresponds to the high inclination asteroids only (see Knežević (2020)), the match is nearly perfect. All the other resonances do not seem to interact with asteroids in the zone, and thus also with families, in a significant way.

## 2.9. Zone 9

Zone 9 is the final region of the asteroid belt in which we are going to tackle the problem of identification and precise positioning of the locally present secular resonances, and of their observable interaction with asteroid families. This zone covers the region between  $a = 3.176$  au and  $a = 3.240$  au, or from beyond the  $5J - 2S - 2A$  three-body MMR with Jupiter and Saturn, to the close vicinity of the powerful  $2 : 1$  MMR with Jupiter, usually considered to represent the outer boundary of the Asteroid Main Belt. The

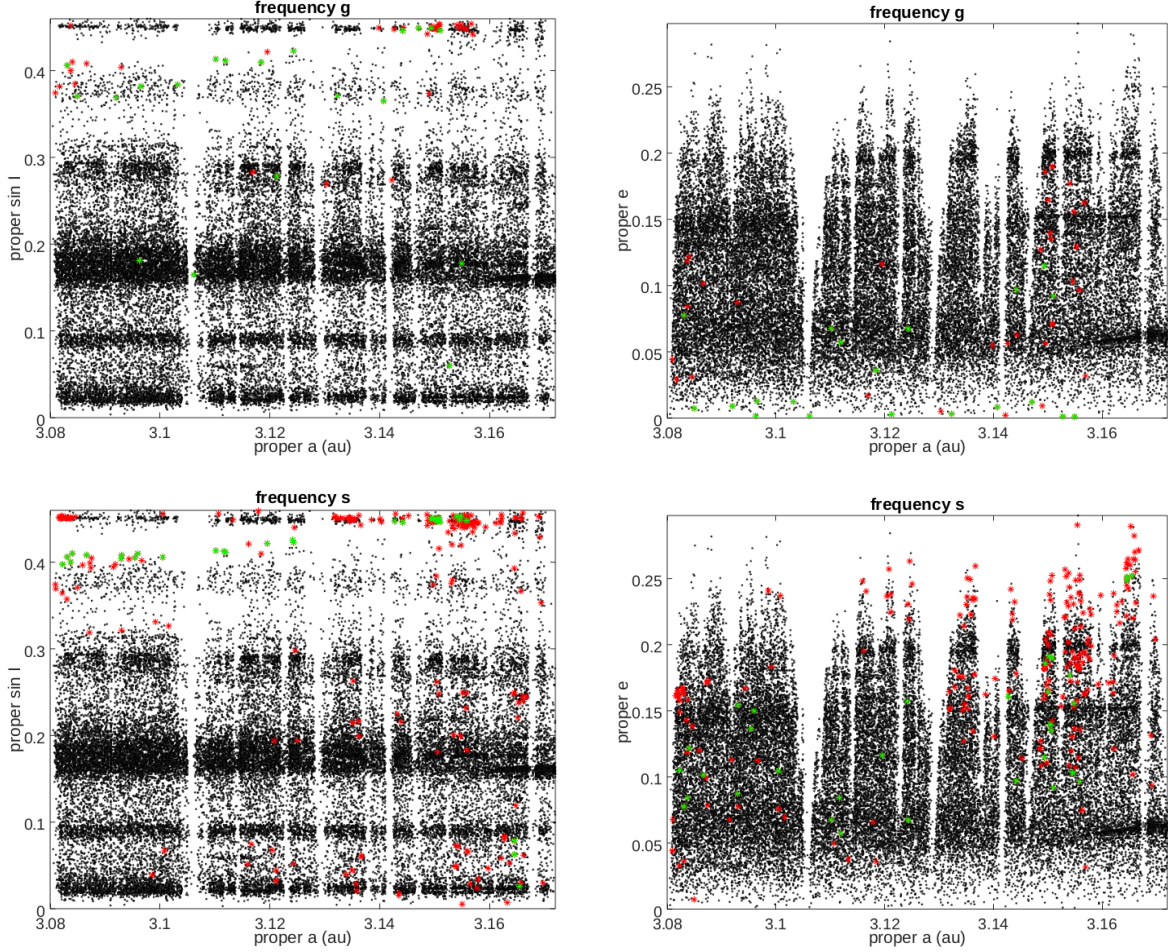


Fig. 16: The same as Fig. 5 but for Zone 8.

upper bound of the region in terms of eccentricity is set to  $e_{\max} = 0.27$  and in terms of inclination to  $\sin I_{\max} = 0.46$  ( $I_{\max} = 27.4$  deg). Because of the proximity to the 2 : 1 MMR and the well known sensitivity of the computation of frequency  $g$  to even a small change in the semimajor axis  $a$ , in the polynomial fit we used a degree 6 polynomial with 42 monomials, that is with a couple of additional terms in semimajor axis like in Zone 4; as many as 13,959 asteroids were used in the fit. The dynamical features of interest are the two nearby three-body MMRs with Jupiter and Saturn:  $7J - 2S + 3A$  at  $a = 3.207$  au and  $9J - 7S - 3A$  at  $a = 3.210$  au, which together create a wide gap in plots due to our pre-fit removal strategy, and also a slightly weaker  $9J - 2S - 4A$  at  $a = 3.224$  au, plus several other resonances of similar strength.

As already mentioned above, more than 20 families extend over the neighboring Zones 8 and 9. On the other hand, there are only a few asteroid families entirely contained within the boundaries of Zone 9. Most of them are either quite small (e.g. Elfriede), in many cases even too small to be considered a con-

firmed non-random grouping. The biggest family in the zone thus turns out to be the a medium size family of (1303) Luthera, with a couple of hundreds of members. Accordingly, also the papers dealing with the families in the zone are but a few, the only one worth mentioning here being the paper by Machuca and Carruba (2012), in which authors discuss the interaction of local asteroids with the web of secular resonances crisscrossing the high inclination region of Luthera family and propose several new possible families and clumps.

Inspection of Table 9 reveals that the accuracy of the fit of frequency  $g$ , with more terms in the polynomial, is similar to or even better than the results obtained for some other zones, in particular for the central Zones 4 and 5. Thus, it can be considered satisfactory, in spite of the aforementioned problems arising with computation of this frequency. The accuracy of the fit for frequency  $s$  is, on the other hand, slightly worse than in other zones, still somewhat better than that for frequency  $g$ , and nevertheless good enough for the purpose of locating the secular resonances. It is the vicinity of the powerful 2 : 1 MMR

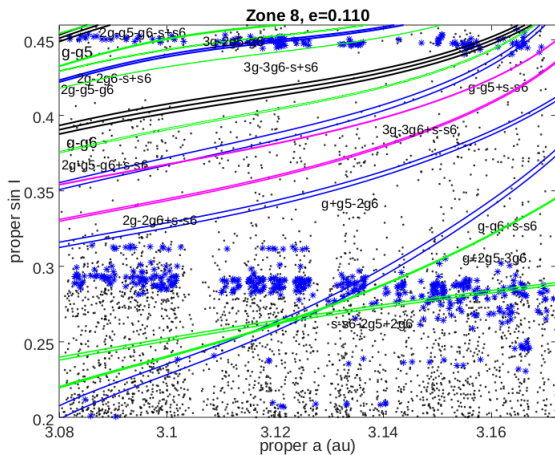


**Fig. 17:** Secular resonances in Zone 8. Resonance positions are computed for  $e = 0.11$ . The colors of the asteroids (only one third of which is shown in the plot) and of the resonant contours are the same as in Fig. 8. Note that in this zone, because of the presence of many resonances in the high inclination zone and none in the zone below  $\sin I = 0.20$ , for clarity we show only the high inclination region. Remarkable families are Ursula and Klumpkea ( $\sin I \sim 0.29$ ), and Euphrosyne ( $\sin I \sim 0.45$ ).

with Jupiter that affects computation of both frequencies (see Fig. 18) in a similar way, thus bringing their error estimates closer to each other.

**Table 9:** The same as in Table 1, but for Zone 9. 13,959 asteroids were used in the fit.

Freq.	$\sigma_{\text{all}}$	$N_{10}$	$\sigma_{10}$	$N_3$	$\sigma_3$
$g$	0.4170	15	0.3709	194	0.2970
$s$	0.2706	19	0.22399	175	0.1749

As a matter of fact, in Fig. 18 one notices a striking similarity of the distribution of asteroids with poorly determined frequencies in both projections - in the  $(a, \sin I)$  and  $(a, e)$  planes - not observed in other zones. In the former plane (left panels), apart from the groups at very high and very low inclination, there is a third group at  $0.3 < \sin I < 0.4$  for which there is no obvious explanation in terms of usual mechanisms, including the resonant ones, thus the only remaining explanation is that these are asteroids belonging to the cluster located at  $a \simeq 3.2$  au, and  $e \simeq 0.25$ , affected in terms of eccentricity by the 2 : 1 resonance (see the right panels). The remaining difference in accuracy of the fit of  $g$  and  $s$  resonances can also be explained by the similar cause if we observe that in the right upper panel the number of cases of deteriorated frequencies, including the “pathological” cases, is significantly larger than in the

lower panel, and that their distribution stretches next to the resonant gap, while in the other case it ends up further away, actually already at the edge of the  $9J - 2S - 4A$  three-body MMR.

To conclude the survey of Zone 9, we show Fig. 19 in which the locations of secular resonances present in this zone are plotted. All the relevant resonances are found in the high inclination region and all but one in the very high inclination region. Hence, they cannot have a significant effect on the dynamics in the zone, nor can affect a large number of asteroids (except, perhaps, some members of the Euphrosyne family protruding into Zone 9). The only resonance at slightly lower inclination of  $\sin I \simeq 0.3$  is a degree 6 resonance  $s - s_6 - 2g_5 + 2g_6$ .

### 3. DISCUSSION AND CONCLUSIONS

In this review we presented a survey of secular resonances in the asteroid Main Belt. We focused on basically four main issues: (i) estimate of accuracy of determination of the perihelion and nodal frequencies ( $g, s$ ) by means of polynomial fit; (ii) identification of dynamical mechanisms responsible for deterioration of the accuracy of results; (iii) determination of positions of all secular resonances up to order four with Jupiter and Saturn and of some of higher order or involving other planets; (iv) interaction of newly positioned secular resonances with known asteroid families.

(i) One can safely say that the accuracy of computation of frequencies, expressed in terms of differences of two sets of values computed independently is in all zones good enough for the purpose of determination of secular resonances’ locations. In Table 10 we summarize the best fit values, as given in Tables 1-9 for individual zones. Obviously, these are always the values obtained after removal of the  $3\sigma$  outliers.

**Table 10:** Summary of the best fit values of frequencies ( $g, s$ ) for the dynamically distinct zones of the asteroid belt.  $N_{\text{fit}}$  gives number of asteroids used in the fit.

Zone	$N_{\text{fit}}$	$g$	$s$
1	6485	0.0872	0.0152
2	16400	0.0299	0.0321
3	91772	0.0678	0.0321
4	87606	0.5276	0.0724
5	56869	0.3490	0.1371
6	20094	0.2644	0.0279
7	36619	0.1997	0.0907
8	38520	0.2720	0.1000
9	13959	0.2970	0.1749

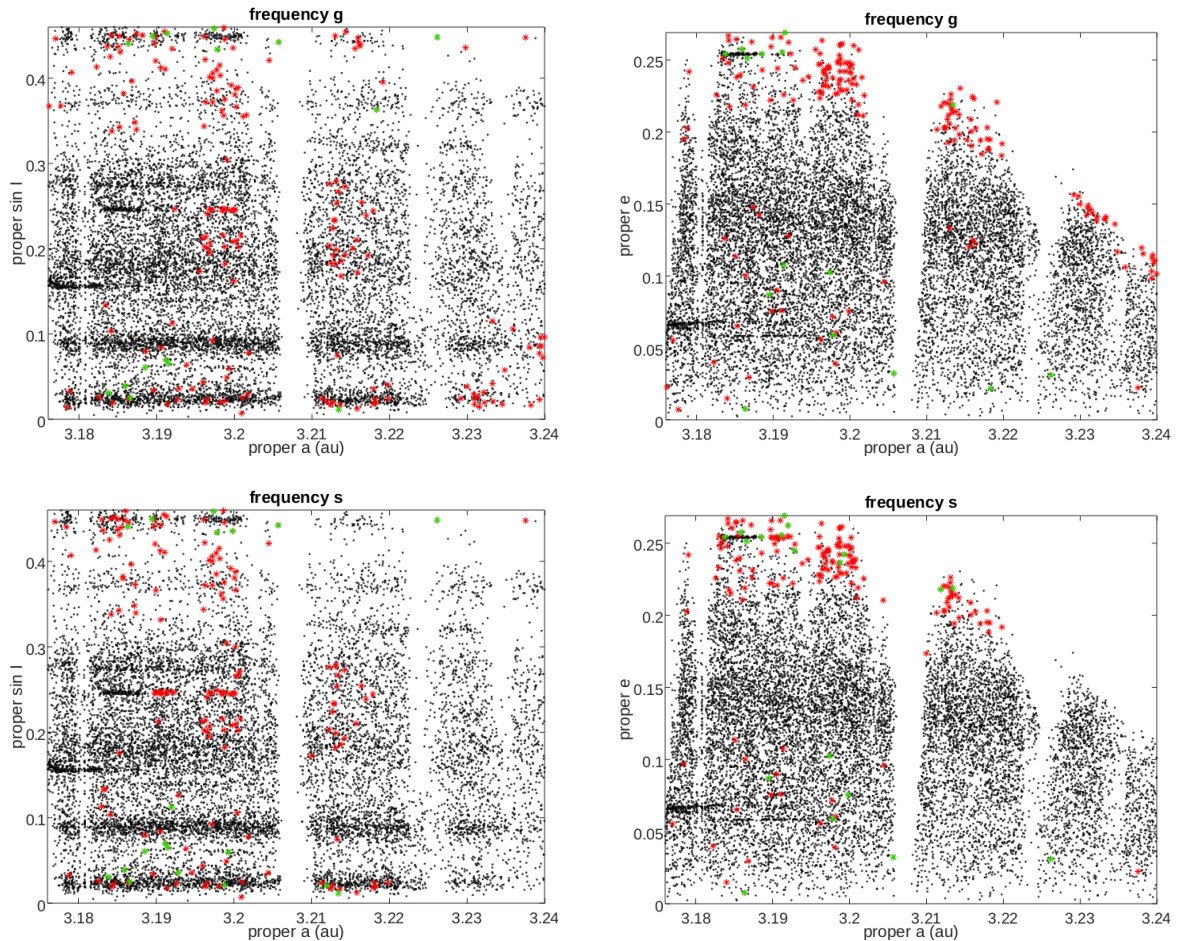


**Fig. 18:** The same as Fig. 5 but for Zone 9.

Even in the worst case (Zone 4, frequency  $g$ ), the standard deviation of the differences is on the order of a half of arcsec/yr, which in terms of the proper inclination corresponds to an uncertainty of the resonance position of several tens of a degree (see e.g. Fig. 3, but one must keep in mind that for each zone and range of proper inclination this can be slightly different). In many cases, on the contrary, in particular for the frequency  $s$ , this standard deviation is less than 0.1 arcsec/yr, which translates into a negligible uncertainty of the position of the resonance.

(ii) The principal dynamical mechanisms affecting the computation of synthetic proper frequencies ( $g, s$ ) are just two: MMRs and secular resonances. The close vicinity of the former, and libration in the latter are in that sense the most effective. In the case of libration it is sometimes even necessary to compute the specially adapted proper elements, the so called resonant proper elements (Morbidelli 1993, Milani et al. 2017), in order to have a meaningful representation of the long term dynamics for such bodies. The problem with resonant elements, however, is that they have to be computed separately for each relevant resonance. Moreover, these elements are not

compatible with the non resonant proper elements computed from the theories based on averaging over slow angles, and cannot be used together with the latter e.g. to identify the families.

Another mechanism, but of a purely technical nature, which causes a serious deterioration of the accuracy of computation of synthetic frequency  $g$  are the “cycle slips” (Knežević 2020), typical of asteroids with extremely low eccentricities and high inclinations. The remedy for this problem is known but not yet applied in practice.

(iii) The positions of secular resonances computed in this work are the most accurate positions one can currently determine using a kind of general approach employed here to simultaneously locate all the resonances in a given dynamical zone. Based on the synthetic proper frequencies and on the new algorithm allowing their computation on a regular grid in the space of proper elements, these positions represent the best available approximations to the real ones, except for the possibility of a dedicated effort to find the most accurate position of a selected resonance by accounting for special properties of the local dynamics.

**Table 11:** Secular resonances in the asteroid belt. The lists for individual zones contain only resonances present in these zones in the  $(a, \sin I)$  plane and involving, with a few exceptions mostly in Zone 1, just Jupiter and Saturn. All resonances up to order four, a significant fraction of the order six resonances, and several order eight ones are considered. Some most remarkable asteroid families in each zone interacting with a resonance of a given order are also indicated.

Zone	Resonances	Families
1	$g - g_3, g - g_4, g - g_5, s - s_4, s - s_6$ $2g - g_5 - g_6, g - g_5 - s + s_6, 2s - s_4 - s_6$ $s - g_5 + g_8 - s_6, s + g_5 - g_8 - s_3$ $2g - 2g_5 + s - s_7, g - g_5 - 2s + 2s_6$ $3g - 2g_5 - g_6, s - g_6 + g_8 - 2s_6 + s_7, s + g_4 - g_6 - 2s_4 + s_7$ $s + 2g_4 - g_5 - g_6 - s_3, s - g_5 + g_6 + s_7 - 2s_8$	Hungaria
2	$g - g_6$ $g - g_5 + s - s_6$ $2g - 2g_6 + s - s_6, 2g - 2g_6 - s + s_6, 2g - g_5 - g_6 - s + s_6$ $3g - 3g_6 + s - s_6, 3g - 3g_6 - s + s_6$	Matterania
3	$g - g_6, s - s_6$ $g - g_5 + s - s_6, g - g_6 - s + s_6, 2g - g_5 - g_6$ $2g - g_5 - g_6 + s - s_6, 2g - g_5 - g_6 - s + s_6$ $2g - 2g_6 + s - s_6, 2g - 2g_6 - s + s_6, 2g - 3g_6 + g_5, g - g_5 + 2s - 2s_6$ $3g - 3g_6 + s - s_6, 3g - 3g_6 - s + s_6$	Svea, Lucienne Phocaea Erigone
4	$g - g_5, g - g_6$ $g + g_5 - 2g_6, g - g_5 + s - s_6, g - g_5 - s + s_6, g - g_6 - s + s_6$ $2g - g_5 - g_6, s - s_6 - g_5 + g_6$ $2g - g_5 - g_6 + s - s_6, 2g - g_5 - g_6 - s + s_6, 2g - 2g_6 + s - s_6$ $3g - 2g_5 - g_6$	Barcelona Astraea, Karma Gersuind Hansa
5	$g - g_5, g - g_6$ $g - g_5 + s - s_6, g - g_5 - s + s_6, g - g_6 + s - s_6, g - g_6 - s + s_6$ $g + g_5 - 2g_6, 2g - g_5 - g_6, s - s_6 - g_5 + g_6$ $2g - 2g_6 + s - s_6, 2g - 2g_6 - s + s_6, 2g - g_5 - g_6 + s - s_6$ $2g - g_5 - g_6 - s + s_6, 3g - 2g_5 - g_6$ $3g - 3g_6 + s - s_6, 3g - 3g_6 - s + s_6$	Tina Padua, Agnia
6	$g - g_6 + s - s_6, g + g_5 - 2g_6, s - s_6 - g_5 + g_6$ $g + 2g_5 - 3g_6, 2g - 2g_6 + s - s_6, s - s_6 - 2g_5 + 2g_6$ $3g - 3g_6 + s - s_6$	4057P - L Koronis
7	$g - g_5 + s - s_6, g - g_6 + s - s_6, g + g_5 - 2g_6$ $g + 2g_5 - 3g_6, 2g - 2g_6 + s - s_6, s - s_6 - 2g_5 + 2g_6$ $3g - 3g_6 + s - s_6$	Eos, Emma, Klytaemnestra
8	$g - g_5, g - g_6$ $2g - g_5 - g_6, g - g_5 + s - s_6, g - g_6 + s - s_6, g + g_5 - 2g_6$ $g + 2g_5 - 3g_6, 2g - 2g_6 + s - s_6, 2g - 2g_6 - s + s_6, 2g - g_5 - g_6 + s - s_6$ $2g - g_5 - g_6 - s + s_6, 3g - 2g_5 - g_6, s - s_6 - 2g_5 + 2g_6$ $3g - 3g_6 + s - s_6, 3g - 3g_6 - s + s_6$	Euphrosyne Hygiea, Ursula, Klumpkea
9	$g - g_6 + s - s_6, g + g_5 - 2g_6$ $g + 2g_5 - 3g_6, 2g - 2g_6 + s - s_6, s - s_6 - 2g_5 + 2g_6$ $3g - 3g_6 + s - s_6$	Luthera

In this paper we included in our investigation all the resonances up to order four, with significant fraction of the order six resonances, and with several order eight ones. The resonant combinations involving fundamental frequencies of Jupiter and Saturn were considered, with a few special cases involving other planets and major asteroids. We note that there are many divisors in the equations of asteroid secular mo-

tion that cannot give rise to resonances, at least as long as the perihelion frequency  $g$  is positive, and the nodal frequency  $s$  is negative, which is the case for the vast majority of asteroids in the main belt.

In Table 11 we list all relevant resonances in each of the considered dynamical zones of the asteroid belt, shown in the corresponding figures like e.g. Fig. 6 for Zone 2 or Fig. 19 for Zone 9.

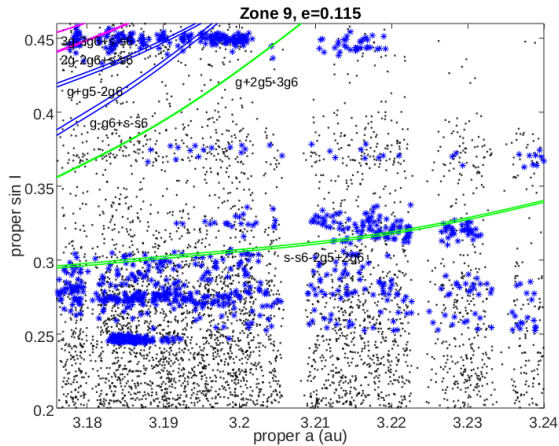


**Fig. 19:** Secular resonances in Zone 9. Resonance positions are computed for  $e = 0.115$ . The colors of the asteroids and resonant contours are the same as in Fig. 8. Note that in this zone too, because of the presence of many resonances in the high inclination zone and none in the zone below  $\sin I = 0.20$ , we show here only the high inclination region.

(iv) In the same table, information is given on the known families having some kind of interaction with secular resonances. The interactions of families with secular resonances are typically not as strong as with the MMRs, but nevertheless, in many cases they are clearly recognizable, even important, and indicated as giving rise to some observed features of the families. Among such resonant features are the existence of family members librating in some secular resonance, increase of the spread of families in the phase space of proper elements, changes of proper elements of family members crossing the secular resonances, secular resonances as dynamical routes, with or without Yarkovsky effect, for the transport of family asteroids, bounding and separating the regions in the Main Belt with a consequence of families ending up in the resonances, creation of gaps or dips, that is regions of lower spatial density of asteroids, etc. Not all secular resonances are, however, equally efficient in creating signatures of their presence in or near the families.

In addition to the above listed items regarding the computation of frequencies and finding the best positions of secular resonances, in this review we also reviewed the recent literature relevant for the topic. Although such a review can never be exhaustive, we argue that we managed to present and discuss a fairly complete sample of works containing the most important published results regarding the secular resonances and asteroid families. We expect this effort to be useful for the reader, either just as an information, or as a valuable resource for future studies.

When the possibilities for future work are in question, we may suggest considering the improvement of the method to compute the frequencies by experimenting with increasing the degree of the fitting poly-

nomial and the number of monomials, at least in the most critical cases (Zone 4), completion of the list of order six secular resonances of some importance for the asteroid dynamics which should be included in future research, consideration of resonances with major planets other than Jupiter and Saturn, etc.

*Acknowledgements* – This review is dedicated to the memory of Andrea Milani. The author acknowledges the financial support through the project F-187 of the Serbian Academy of Sciences and Arts.

## REFERENCES

- Bolin, B. T., Delbo, M., Morbidelli, A. and Walsh, K. J. 2017, *Icarus*, **282**, 290
- Bottke, W. F., Vokrouhlický, D., Broz, M., Nesvorný, D. and Morbidelli, A. 2001, *Science*, **294**, 1693
- Brož, M., Morbidelli, A., Bottke, W. F., et al. 2013, *Astron. Astrophys.*, **551**, A117
- Carruba, V. 2009, *Mon. Not. R. Astron. Soc.*, **395**, 358
- Carruba, V. and Barletta, W. 2019, *Planet. Space Sci.*, **165**, 10
- Carruba, V. and Morbidelli, A. 2011, *Mon. Not. R. Astron. Soc.*, **412**, 2040
- Carruba, V. and Ribeiro, J. V. 2020, *Planet. Space Sci.*, **182**, 104810
- Carruba, V., Michtchenko, T. A., Roig, F., Ferraz-Mello, S. and Nesvorný, D. 2005, *Astron. Astrophys.*, **441**, 819
- Carruba, V., Aljbaae, S. and Souami, D. 2014a, *Astrophys. J.*, **792**, 46
- Carruba, V., Domingos, R. C., Huaman, M. E., Santos, C. R. d. and Souami, D. 2014b, *Mon. Not. R. Astron. Soc.*, **437**, 2279
- Carruba, V., Aljbaae, S. and Winter, O. C. 2016a, *Mon. Not. R. Astron. Soc.*, **455**, 2279
- Carruba, V., Domingos, R. C., Aljbaae, S. and Huaman, M. 2016b, *Mon. Not. R. Astron. Soc.*, **463**, 705
- Carruba, V., Nesvorný, D. and Aljbaae, S. 2016c, *Icarus*, **271**, 57
- Carruba, V., Vokrouhlický, D. and Novaković, B. 2018, *Planet. Space Sci.*, **157**, 72
- Čuk, M., Gladman, B. J. and Nesvorný, D. 2014, *Icarus*, **239**, 154
- Erasmus, N., McNeill, A., Mommert, M., et al. 2019, *Astrophys. J. Suppl. Ser.*, **242**, 15
- Gallardo, T. 2014, *Icarus*, **231**, 273
- Huaman, M., Roig, F., Carruba, V., Domingos, R. C. and Aljbaae, S. 2018, *Mon. Not. R. Astron. Soc.*, **481**, 1707
- Knežević, Z. 2016, in IAU Symposium, Vol. 318, Asteroids: New Observations, New Models, ed. S. R. Chesley, A. Morbidelli, R. Jedicke and D. Farnocchia, 16–27
- Knežević, Z. 2017, *Serb. Astron. J.*, **195**, 1
- Knežević, Z. 2020, *Mon. Not. R. Astron. Soc.*, **497**, 4921
- Knežević, Z. and Milani, A. 2000, *Celest. Mech. Dyn. Astron.*, **78**, 17
- Knežević, Z. and Milani, A. 2019, *Celest. Mech. Dyn. Astron.*, **131**, 27

- Knežević, Z., Milani, A., Farinella, P., Froeschle, C. and Froeschle, C. 1991, *Icarus*, **93**, 316
- Knežević, Z., Milani, A., Cellino, A., et al. 2014, in IAU Symposium, Vol. 310, Complex Planetary Systems, Proceedings of the International Astronomical Union, 130–133
- Lucas, M. P., Emery, J. P., MacLennan, E. M., et al. 2019, *Icarus*, **322**, 227
- Machuca, J. F. and Carruba, V. 2012, *Mon. Not. R. Astron. Soc.*, **420**, 1779
- Masiero, J. R., Carruba, V., Mainzer, A., Bauer, J. M. and Nugent, C. 2015, *Astrophys. J.*, **809**, 179
- McEachern, F. M., Čuk, M. and Stewart, S. T. 2010, *Icarus*, **210**, 644
- Michel, P. and Froeschlé, C. 1997, *Icarus*, **128**, 230
- Milani, A. 1994, in IAU Symposium, Vol. 160, Asteroids, Comets, Meteors 1993, ed. A. Milani, M. di Martino and A. Cellino, 159
- Milani, A. and Knežević, Z. 1990, *Celest. Mech. Dyn. Astron.*, **49**, 347
- Milani, A. and Knežević, Z. 1992, *Icarus*, **98**, 211
- Milani, A. and Knežević, Z. 1994, *Icarus*, **107**, 219
- Milani, A., Knežević, Z., Novaković, B. and Cellino, A. 2010, *Icarus*, **207**, 769
- Milani, A., Cellino, A., Knežević, Z., et al. 2014, *Icarus*, **239**, 46
- Milani, A., Spoto, F., Knežević, Z., Novaković, B. and Tsirvoulis, G. 2016, in Asteroids: New Observations, New Models, ed. S. R. Chesley, A. Morbidelli, R. Jedicke and D. Farnocchia, Vol. 318, 28–45
- Milani, A., Knežević, Z., Spoto, F., et al. 2017, *Icarus*, **288**, 240
- Milani, A., Knežević, Z., Spoto, F. and Paolicchi, P. 2019, *Astron. Astrophys.*, **622**, A47
- Morbidelli, A. 1993, *Icarus*, **105**, 48
- Nesvorný, D. and Morbidelli, A. 1998, *Astron. J.*, **116**, 3029
- Nesvorný, D., Brož, M. and Carruba, V. 2015, Identification and Dynamical Properties of Asteroid Families, 297–321
- Novaković, B., Maurel, C., Tsirvoulis, G. and Knežević, Z. 2015, *Astrophys. J. Lett.*, **807**, L5
- Novaković, B., Tsirvoulis, G., Marò, S., Djošović, V. and Maurel, C. 2016, in Asteroids: New Observations, New Models, ed. S. R. Chesley, A. Morbidelli, R. Jedicke and D. Farnocchia, Vol. 318, 46–54
- Oszkiewicz, D., Kankiewicz, P., Włodarczyk, I. and Kryszczyńska, A. 2015, *Astron. Astrophys.*, **584**, A18
- Pavela, D., Novaković, B., Carruba, V. and Radović, V. 2021, *Mon. Not. R. Astron. Soc.*, **501**, 356
- Spoto, F., Milani, A. and Knežević, Z. 2015, *Icarus*, **257**, 275
- Tsirvoulis, G. 2019, *Mon. Not. R. Astron. Soc.*, **482**, 2612
- Tsirvoulis, G. and Novaković, B. 2016, *Icarus*, **280**, 300
- Tsirvoulis, G., Morbidelli, A., Delbo, M. and Tsiganis, K. 2018, *Icarus*, **304**, 14
- Vokrouhlický, D. and Brož, M. 2002, in Modern Celestial Mechanics: From Theory to Applications, ed. A. Celletti, S. Ferraz-Mello and J. Henrard, 467–472
- Vokrouhlický, D., Brož, M., Morbidelli, A., et al. 2006, *Icarus*, **182**, 92
- Vokrouhlický, D., Bottke, W. F. and Nesvorný, D. 2017a, *Astron. J.*, **153**, 172
- Vokrouhlický, D., Pravec, P., Durech, J., et al. 2017b, *Astron. Astrophys.*, **598**, A91
- Warner, B. D., Harris, A. W., Vokrouhlický, D., Nesvorný, D. and Bottke, W. F. 2009, *Icarus*, **204**, 172
- Williams, J. G. and Faulkner, J. 1981, *Icarus*, **46**, 390

## ПРЕГЛЕД СЕКУЛАРНИХ РЕЗОНАНЦИ У АСТЕРОИДНОМ ПОЈАСУ

Z. Knežević

*Serbian Academy of Sciences and Arts,  
Kneza Mihaila 35, 11000 Belgrade, Serbia*E-mail: *zoran.knezevic@sanu.ac.rs*

УДК 523.44–32

*Прегледни рад по позиву*

Користећи недавно развијени синтетички метод за израчунавање секуларних фреквенција астероида (Knežević and Milani, 2019), у овом раду приказујемо преглед локација секуларних резонанци у 9 динамички различитих зона у астероидном појасу. Одредили смо положаје свих резонанци до четвртог реда, већег дела резонанци шестог реда, као и неколико резонанци осмог реда, графички их приказали у простору сопствених елемената кретања и анализирали њихов утицај на локалну динамику и структуру и облик блиских сударних фамилија астероида. Разматране су само резонантне комбинације са фундаменталним фреквенцијама Јупитера и Сатурна, уз неколико специјалних случајева који су укључивали друге планете и највеће астеро-

иде. Утврђено је да је тачност полиномског фитовања у сврху одређивања фреквенција довољна за потребе одређивања положаја секуларних резонанци. То је омогућило прецизну идентификацију динамичких механизма који утичу на рачун фреквенција (близина резонанци у средњем кретању и либрација у секуларним резонанцама), односно “прескакања циклуса” као основног техничког проблема који доводи до “кварења” резултата. За сваку зону су представљени готово сви важнији недавно објављени радови који се баве интеракцијом секуларних резонанци и астероидних фамилија лоцираних у датој зони. На крају, неколико речи је посвећено могућностима за будући рад.